Inaugural dissertation
for
obtaining the doctoral degree
of the
Combined Faculty of Mathematics, Engineering and Natural Sciences
of the
Ruprecht - Karls - University Heidelberg

Presented by
M.Sc. Juliane Poelchen
born in: Leipzig, Germany
Oral examination: 05.06.2023

Generation of melanoma antigen-specific $CD8^+$ T cells from human induced pluripotent stem cells for adoptive cell therapy

Referees: Prof. Dr. Viktor Umansky
Prof. Dr. Jochen Utikal

Declarations according to § 8 (3) b) and c) of the doctoral degree regulations:

b) I hereby declare that I have written the submitted dissertation myself and in this process have used no other sources or materials than those expressly indicated,

c) I hereby declare that I have not applied to be examined at any other institution, nor have I used the dissertation in this or any other form at any other institution as an examination paper, nor submitted it to any other faculty as a dissertation.

Heidelberg, 12.04.2023

Juliane Poelchen

Parts of this thesis have been published in:

Conferences and workshop presentations

Juliane Poelchen, Daniel Novak, Viktor Umansky, Jochen Utikal
Poster: ”Generation of CD8+ T cells from induced pluripotent stem cells for immunotherapy”
DKFZ PhD Poster Session, November 2020, Heidelberg, Germany

Juliane Poelchen, Daniel Novak, Jochen Utikal
Poster: ”Generation of CD8+ T cells from induced pluripotent stem cells for immunotherapy”
International PhD Student Conference Europe, June 2021, Virtual

Juliane Poelchen, Daniel Novak, Jochen Utikal
Scheme Your Project: ”Generation of CD8+ T cells from induced pluripotent stem cells for immunotherapy”
Ph.D. Virtual Retreat, June 2021, Virtual

Juliane Poelchen, Daniel Novak, Pierre Guermonprez, Viktor Umansky, Jochen Utikal
Poster and Flashtalk: ”Generation of CD8+ T cells from induced pluripotent stem cells for immunotherapy”
Hallmarks of Skin Cancer Conference (HoSC), November 2021, Virtual

Contents

List of Figures

List of Tables

Abstract

Adoptive cell therapy using tumor antigen-specific $CD8^+$ T cells is a promising approach to treat patients with advanced or metastasizing cancer including malignant melanoma. The general procedure is based on the isolation, *in vitro* stimulation and expansion of tumor-infiltrating lymphocytes (TILs). These activated and expanded TILs, which are specific for common tumor antigens are then transferred back into the patients to attack and neutralize cancer cells. However, current studies report disease relapse in treated patients because of T cell exhaustion after ongoing TCR stimulation resulting in a decreased effector function and a loss of their replicative capacity.

The use of induced pluripotent stem cells (iPSCs) as a source for the generation of "off-the-shelf" $CD8^+$ T cells could enable T cell-based immunotherapy on a large scale. Similar to embryonic stem cells, iPSCs have the potential to give rise to nearly unlimited amounts of any cell type, including $CD8^+$ T cells. The aim of this project was to develop strategies for the *in vitro* generation of melanoma antigen-specific $CD8^+$ T cells from human iPSCs.

First, iPSCs were transfected with S/MAR DNA vectors coding for a T cell receptor (TCR) against MART-1 or a chimeric antigen receptor (CAR) directed against MCSP. S/MAR DNA vectors are effective gene delivery systems since they contain a scaffold/matrix attachment region, which binds to the nuclear matrix and ensures a persistent gene expression over hundreds of cell divisions. The transfection of iPSCs with the S/MAR DNA vector did not alter the gene expression of the pluripotency genes NANOG and OCT4 as well as other T cell-related differentiation genes.

Next, a 2D co-culture system with OP9 murine stromal cells was used to facilitate the differentiation of $CD34^+$ hematopoietic stem and progenitors cells (HSPCs) from iPSCs. Further differentiation of $CD34^+$ HSPCs into $CD4^+CD8^+$ double-positive (DP) T cells was achieved by long-term co-culture with bioengineered OP9 stromal cells expressing T cell-specific cytokines like FLT3-ligand, CXCL12 and SCF as well as the Notch ligand DLL4 and supplementation of the growth medium with recombinant IL7.

Since clinical applications require clean populations of effector T cells without contamination with murine cells, the stromal cell based co-culture system was replaced with a commercially available differentiation kit. Following the manufacturer's instructions, I was able to generate a limited amount of $CD8^+$ single-positive (SP) T cells. Flow cytometric analysis of common T cell markers revealed a low CD3 expression in generated T cells but a persistent MART-1 TCR or MCSP CAR expression, respectively. In comparison to $CD4^+CD8^+$ DP T cells, $CD8^+$ SP T cells demonstrated

the capability to produce cytokines, showed degranulation capacity after stimulation and exhibited cytotoxic effects against melanoma cell lines.

Hence, these findings revealed the possibilities as well as the challenges connected with the use of human iPSCs for the generation of $CD8^+$ T cells. However, the use of S/MAR DNA vectors and novel differentiation strategies could enable further clinical applications in cancer treatment and help to improve common immunotherapies for melanoma patients.

Zusammenfassung

Bei der adoptiven T-Zelltherapie mit tumorspezifischen $CD8^+$ T-Zellen handelt es sich um eine innovative Therapiemethode für Krebspatienten im fortgeschrittenen Stadium. Dabei werden tumorinfiltrierende Lymphozyten (TILs) aus dem Körper des Patienten isoliert, stimuliert und expandiert bevor sie dem Patienten als personalisierte Therapie wieder zurückgeführt werden. Neuerdings gibt es jedoch Studien, die von späteren Krankheitsrückfällen trotz erfolgreicher anfänglicher Therapie berichten. Diese Rückfälle lassen sich auf einen Erschöpfungszustand der T-Zellen durch andauernde T-Zell Rezeptorstimulation zurückführen und einer damit einhergehenden verminderten T-Zell Proliferation.

Die Verwendung von induzierten pluripotenten Stammzellen als Ausgangmaterial für die Herstellung von $CD8^+$ T-Zellen wäre eine Möglichkeit, T-zellbasierte Immuntherapien in großem Maßstab zu revolutionieren. IPS-Zellen besitzen die gleichen Eigenschaften wie embryonale Stammzellen und lassen sich somit in jeden beliebigen Zelltyp umwandeln. Das Ziel dieses Projektes bestand darin, Strategien für die Herstellung von tumorspezifischen $CD8^+$ T-Zellen aus humanen iPS-Zellen zu entwickeln.

Dazu wurden die iPS-Zellen zunächst mit einem S/MAR DNA Vektor transfiziert, der einen melanomspezifischen T-Zellrezeptor bzw. einen chimären Antigenrezeptor kodiert. Die Transfektion mit den S/MAR Vektoren hatte keinen Einfluss auf die Expression der Pluripotenzgene NANOG und OCT4 und auf wichtige Gene der T-Zelldifferenzierung.

Im nächsten Schritt wurden mithilfe von murinen OP9 Stromazellen $CD34^+$ hematopoetische Stamm- und Vorläuferzellen (HSPCs) erzeugt. Für die weitere Differenzierung in Richtung $CD4^+CD8^+$ DP T-Zellen wurden genetisch manipulierte OP9 Zellen verwendet, welche T-zellspezifische Cytokine wie CXCL12, SCF, FLT3-Liganden und den NOTCH Liganden DLL4 exprimieren.

Da für weitere potentielle klinische Anwendungen keine Zellen murinen Ursprungs in der Endpopulation enthalten sein dürfen, wurde das Co-Kultivierungssystem im weiteren Verlauf durch ein kommerziell verfügbares Differenzierungsset ersetzt. Mithilfe dieses Sets war es möglich, $CD8^+$ SP T-Zellen in geringen Maßen zu generieren. Durchflusszytometrische Analysen bekannter T Zellmarker zeigten eine geringe CD3 Expression. Die Expression des MART-1 TCRs bzw. des MCSP CARs war hingegen auch im $CD8^+$ SP T Zellstadium vorhanden. Im Vergleich zu den $CD4^+CD8^+$ DP T-Zellen produzierten die $CD8^+$ SP T-Zellen Zytokine, wiesen die Fähigkeit zur Degranulation auf und es ließen sich zytotoxische Effekte gegenüber Melanomzellen feststellen.

Die gewonnenen Erkenntnisse zeigen mögliche Perspektiven, aber auch bestehende Herausforderungen bei der Herstellung von $CD8^+$ T-Zellen aus humanen iPS-Zellen auf. Weiterführende Studien, die zur Entwicklung von neuen Vektorsystemen in Kombination mit ausgereifteren Differenzierungssystemen beitragen, sind die Voraussetzung, um zukünftige klinische Anwendungen als Immuntherapien für Melanompatienten zu ermöglichen.

List of abbreviations

3D	three-dimensional
ACT	adoptive cell therapy
Akt	protein kinase B
ANOVA	One-way analysis of variance
APCs	antigen presenting cells
ATOs	artificial thymic organoids
bFGF	basic fibroblast growth factor
BM	bone marrow
BRAF	B-Raf proto-oncogene, serine/threonine kinase
bp	base pair
CAG	chicken beta-actin promoter
CD	cluster of differentiation
CDKN2A	cyclin-dependent kinase inhibitor 2 A
cDNA	Complementary DNA
CCL25	C-C motif chemokine ligand 25
CCR9	C-C chemokine receptor type 9
CXCL12	C-X-C motif chemokine ligand 12
CXCR4	C-X-C motif chemokine receptor 4
CGAs	cancer germline antigens
CNRS	Centre national de la recherche scientifique
CTLA-4	cytotoxic T lymphocyte-associated molecule-4
DAPI	4′,6-diamidino-2-phenylindole

DC	dendritic cell
DKFZ	Deutsches Krebsforschungszentrum
DLL	delta like canonical Notch ligand
DMEM	Dulbeccos's Modified Eagle Medium
DNA	deoxyribonucleic acid
DN	double negative
DP	double positive
DTIC	Dacarbazine
E.coli	Escherichia coli
E40	Element40
EB	embryoid body
ECM	extracellular matrix
EDTA	Ethylenediaminetetraacetic acid
EGFR	epidermal growth factor receptor
EMT	epithelial-to-mesenchymal transition
ERK	extracellular signal-regulated kinase
ESCs	embryonic stem cells
FACS	fluorescence-activated cell sorting
FCS	fetal calf serum
FDA	Food and Drug Administration
FLT3-L	Fms-related tyrosine kinase 3 Ligand
FMO	Fluorescence Minus One
FOXN1	Forkhead box protein N1
GOI	gene of interest

gp100	glycoprotein 100
GvHD	graft-versus-host disease
HEPES	2-[4-(2-hydroxyethyl)piperazin-1-yl]ethanesulfonic acid
HLA	human leukocyte antigen
HSPCs	hematopoietic stem and progenitor cells
HSV-1	herpes simplex virus 1
ICI	immune checkpoint inhibitor
IFN	interferon
IL	interleukin
iPSCs	Induced pluripotent stem cells
Klf4	Krüppel-like factor 4
LAG-3	lymphocyte activation gene-3
LB	lysogeny broth
MACS	magnetic-activated cell sorting
MAGE	melanoma-associated antigen
MAPK	mitogen-activated protein kinase
MART-1	Melanoma-associated antigen recognized by T cells
MCSP	melanoma-associated chondroitin sulfate proteoglycan
MEFs	mouse embryonic fibroblasts
MHC	major histocompatibility complex
MEM	Minimum Essential Medium
mRNA	Messenger RNA
MSCs	mesenchymal stromal cells
NEAA	non-essential amino acids

NK	natural killer
NRAS	Neuroblastoma RAS viral oncogene homolog
NYESO-1	New York esophageal squamous cell carcinoma-1
Oct4	octamer-binding transcription factor 4
OS	overall survival
PBMCs	peripheral blood mononuclear cells
PBS	Phosphate-buffered saline
PCR	polymerase chain reaction
PD-L1	Programmed cell death ligand-1
PD1	programmed cell death 1
PDGFRb	Platelet-derived growth factor receptor beta
pen/strep	penicillin/streptomycin
PFS	progression free survival
PI	propidium iodide
PI3K	phosphoinositide-3-kinase
PMA	phorbol myristate acetate
PSCs	pluripotent stem cells
PVDF	polyvinylidene difluoride
qRT-PCR	real time quantitative PCR
RNA	ribonucleic acid
ROCK	Rho-associated protein kinase
RT	room temperature
SCF	stem cell factor
SEM	standard error of the mean

S/MAR scaffold/matrix attachment region

Sox2 sex-determining region Y-box 2

SP single positive

T-VEC Talimogene laherparepvec

TCR T cell receptor

TECs Thymic epithelial cells

TERT telomerase reverse transcriptase

TILs tumor-infiltrating lymphocytes

TIM-3 T cell immunoglobulin and mucin-domain containing-3

TIGIT T-cell immunoreceptor with immunoglobulin and ITIM domains

Tregs regulatory T cells

UCB umbilical cord blood

US United States

UV ultra violet

WT wild type

1 Introduction

1.1 Malignant Melanoma

1.1.1 Overview

Melanoma is the most aggressive and deadliest form of skin cancer. It accounts for the majority of all skin cancer-related deaths, although it just represents around 1 % of all malignant skin tumors [1]. In the last 30 years, the incidence of new melanoma cases increased tremendously with more than 320.000 new diagnosed cases in 2020 worldwide [2, 3]. Melanoma mainly affects the Caucasian population with a 20 times higher risk than African Americans. Therefore, the highest incidence rates for melanoma are found in Australia, New Zealand and Denmark [4]. The overall risk of developing melanoma during life ranges between 2.6 % for Whites and 0.1 % for Blacks [5]. However, several factors as the exposure to UV light during sun bathing or indoor tanning or a past with frequent sunburns increase the risk for developing melanoma in the course of a lifetime. Other personal factors including a fair skin with freckles or light hair color, a great number of nevi (> 25), a family history of melanoma or other skin cancers, a weak immune system and childhood cancer also contribute to a higher risk for melanoma. Additionally, the age, sex and host genome plays a role, too [6, 7]. While patients with localized (stage 1) melanoma have a good prognosis and a 5-year survival rate of 99 %, about 30 % of the patients develop metastases in different organs after primary tumor excision. If the tumor has already spread to distant sites of the body (stage $\geq$3) the 5-year survival rate decreases to less than 30 % since common treatment methods do not significantly improve the survival of patients [8, 9].

1.1.2 Development

The occurrence of melanoma is the result of gene mutations in the pigment producing cells of the skin, the melanocytes. Melanocytes are neural crest-derived cells, which are mainly found in the basilar epidermis of the human skin where to their progenitors migrate during embryonic development. However, low amounts of melanocytes are also present in hair follicles and meninges, in the uveal and anogenital tract [10, 11]. Their main function is the production of melanin pigment for the neighboring keratinocytes, which protects the cells deoxyribonucleic acid (DNA) from being damaged by ultra violet (UV) radiation. However, excessive UV radiation and other intrinsic

factors can still cause DNA damage and replication errors finally leading to melanocytic transformation which is a multistage process [10, 12, 13]. It is common that melanomas appear *de novo* and are not restricted to pre-existing nevi but instead derive from clinically undetectable lesions.

Acquiring a so-called initiating driver mutation is the first step of the transformation process of melanocytes. The most common mutations affect genes of key signaling pathways like the mitogen-activated protein kinase (MAPK) pathway regulating cell proliferation or the phosphoinositide-3-kinase (PI3K)/protein kinase B (Akt) pathway for controlling cell growth and metabolism [10]. 40-50 % of the melanomas carry a mutation of the B-Raf proto-oncogene, serine/threonine kinase (BRAF) gene followed by Neuroblastoma RAS viral oncogene homolog (NRAS) with 15-20 % and NF1 with 10-15 %. Although activating mutations of BRAF lead to nevus development by (limited) expansion of melanocytes, additional genetic alterations are necessary for the progression towards a cancerous BRAF-mutated phenotype [14]. The acquisition of secondary and tertiary mutations in the telomerase reverse transcriptase (TERT) promoter region or in cyclin-dependent kinase inhibitor 2 A (CDKN2A) gene might lead to the emergence of melanoma *in situ*, which is restricted to the epidermis and can persist for many years until it becomes invasive. A melanoma reaches the invasive state as soon as the cells leave the epidermis and infiltrate the adjacent mesenchymal tissue. The last stage of melanoma development is the metastatic melanoma in which the cells leave the original site and colonize distant sites of the body as well as different tissues [10]. Usually, melanoma metastases are found in the tumor draining lymph nodes first before appearing in organs like liver, lung or brain. During the step of metastasis melanoma cells undergo the so called epithelial-to-mesenchymal transition (EMT). This process goes along with a switch towards a more migratory, invasive phenotype [12].

1.1.3 Treatment options

Despite a worldwide increase in newly diagnosed melanoma cases every year, the lethality is decreasing. A milestone in the treatment of melanoma was the invention of targeted therapy and checkpoint immunotherapy in the last 10 years. However, since more than 90 % of the patients are diagnosed in early stages with localized melanoma surgery is still the primary treatment method [1, 15]. Current surgical approaches are very precise, less invasive and show a low morbidity [15]. In patients with higher stage resected melanoma adjuvant therapy like targeted therapy is recommended to reduce the risk of recurrence. In general, patients with advanced stages or metastasized melanoma require additional treatment including chemotherapy, radiotherapy, targeted therapy and immunotherapy.

1.1.3.1 Chemotherapy and Radiotherapy

Until 2011, chemotherapy was considered the standard therapy for metastatic melanoma patients. Dacarbazine (DTIC), which was approved in 1974 by the United States (US) Food and Drug Administration (FDA), is an alkylating agent that is administered intravenously. DTIC causes DNA damage by methylating nucleic acids and therefore leading to cell death and growth arrest of tumor cells. However, besides an improved clinical response a significant improved overall survival (OS) of DTIC treated patients was not reported. Similar effects were also found for the chemotherapeutic temozolomide, which is the prodrug of DTIC and used as an alternative that can be administered orally [1, 16, 17]. Other chemotherapeutics comprise the nitrosoureas carmustine and lomustine as well as carboplatin/taxanes including paclitaxel and docetaxel [18]. Due to the low response rates of patients to single chemotherapy, combinations with immunotherapy like interferon (IFN)-α and interleukin (IL)-2 were used as additional treatment strategy. However, this so-called biochemotherapy is associated with a high toxicity and did not result in the desired improvement of OS of the patients. Especially with the development of targeted and immune checkpoint therapy, biochemotherapy is mainly used as a palliative treatment strategy for patients with late stage progressive and relapsed melanomas [1, 18].

In comparison to chemotherapy, radiotherapy is rarely applied as the primary treatment method rather in combination with targeted therapy or immunotherapy [1].

1.1.3.2 Targeted therapy

A high percentage of melanomas harbors mutations in genes, which encode proteins that are involved in signaling pathways and regulate proliferation, cell cycle and apoptosis. The identification of specific inhibitors for these proteins involved in the constitutive activation of those pathways enabled a promising approach for the treatment of advanced or metastatic melanoma patients, the so-called targeted therapy [19]. Among all the drivers of melanomagenesis, the serine–threonine kinase BRAF belongs to the most commonly mutated genes with a frequency of 50 %. BRAF is part of the RAS–RAF–MEK–ERK MAPK pathway and to this day more than 300 different mutations have been identified. The most frequent mutation results in th substitution of amino acid 600 ($BRAF^{V600E}$) leading to a constant activation of the protein BRAF and therefore to an increased melanoma cell proliferation through constitutive MAPK signaling [19]. Vemurafenib (PLX4032) was the first FDA approved BRAF inhibitor in 2011 followed by dabrafenib (GSK2118436) two years later. Compared to chemotherapy, the treatment with vemurafenib or dabrafenib resulted in an increased progression free survival (PFS) and OS of melanoma patients [20, 21]. However, the

success of current targeted therapies for melanoma patients is mainly limited by two different factors. First, despite having a BRAF mutation not all patients respond to the inhibitors and second, patients easily develop resistance through reactivation of the MAPK signaling pathway. Reasons for that are mutations of downstream targets like MEK, extracellular signal-regulated kinase (ERK) as well as CDKN2A or the activation of PI3K/AKT/mTOR signaling. In addition, an increased expression of receptor tyrosine kinases like epidermal growth factor receptor (EGFR) and Platelet-derived growth factor receptor beta (PDGFRb) or the presence of alternatively spliced variants of BRAF can lead to reactivation [21, 22]. Therefore, the combined inhibition of BRAF and MEK, which is the downstream target of BRAF in the MAPK signaling pathway, is nowadays the targeted therapy option for the treatment of melanoma patients since it significantly improves PFS and OS compared to BRAF monotherapy [21]. Three different combinations have been approved by the FDA so far: dabrafenib + trametinib, vemurafenib + cobimetinib and encorafenib + binimetinib [22]. Nevertheless, extensive research is still going on to find more eficient combinations, which could further improve the clinical outcome for melanoma patients.

1.1.3.3 Immunotherapy

The immune system plays a major role in the surveillance of tumor development and progression. However, tumor cells have developed a range of mechanisms to escape immune surveillance, which of course impairs the protective function of the immune system. These mechanisms include the activation of regulatory pathways that act immunoinhibitory, the recruitment of immunosuppressive cell populations or an altered antigen expression [23]. Therefore, immunotherapies, which exploit the interaction between immune cells and tumor cells are novel approaches for the treatment of melanoma. Several strategies have been developed in the last decade to specifically target cancer cells on the one hand and increase the effector function of immune cells on the other hand.

Oncolytic viruses

In 2015, the first oncolytic virus therapy was approved by the FDA for the treatment of unresectable metastatic melanoma [24, 25]. Talimogene laherparepvec (T-VEC), a genetically modified herpes simplex virus 1 (HSV-1), was generated to specifically lyse tumor cells in order to trigger the release of tumor-specific antigens. Injection of the virus directly into the metastatic melanoma nodules promotes anti-tumor immunity by inducing the activation of melanoma specific T cell responses [21, 24]. The application of T-VEC showed remarkable clinical benefit and improved OS of melanoma patients [23].

Cytokines

The use of cytokines for the treatment of melanoma started in 1995 with the approval of IFN-α for adjuvant therapy [21]. IFN-α belongs to the family of type I interferons which play important roles in natural cancer immunosurveillance and antitumor immunity. On the one hand IFN-α induces the elimination of tumor cells through the induction of apoptosis and senescence and on the other hand it enhances T-cell cytotoxicity and dendritic cell (DC) stimulation [23, 26]. Nowadays IFN-α is less commonly administered as monotherapy due to its strong adverse effects but rather in combination with other immunotherapies such as adoptive T cell transfer or targeted therapies [21, 23]. IL-2 was officially approved 3 years later for the treatment of metastatic melanoma. It is primarily produced by antigen-simulated cluster of differentiation (CD)4^+ T cells but also by $CD8^+$ T cells, natural killer (NK) cells, and DCs. Among others, IL-2 enhances the cytotoxic effect of $CD8^+$ T and NK cells and modulates T cell differentiation programs [27]. Although therapy with IL-2 induced tumor regression, it showed limited improvement of patients OS but instead severe adverse effects and high toxicity. For that reason, IL-2 is no longer administered as monotherapy for metastatic melanoma patients but rather in combination with other anticancer immunotherapies [27].

Immune checkpoint inhibitors

The discovery of immune checkpoints as possible therapeutic targets opened up completely new treatment opportunities for cancer patients. The first approved immune checkpoint inhibitor (ICI) on the market was ipilimumab in 2011. Ipilimumab, a monoclonal antibody, prevents the inhibition of T cells by binding cytotoxic T lymphocyte-associated molecule-4 (CTLA-4) which is expressed on the surface of T cells and acts as co-inhibitory molecule to suppress T cell activation [23, 28, 29]. The blockade of CTLA-4 using ipilimumab is associated with an enhanced T cell function and leads to an increased OS of melanoma patients [30]. Pembrolizumab and nivolumab were approved in 2014 and target the programmed cell death 1 (PD1) receptor, which is overexpressed on exhausted $CD8^+$ T cells as reaction towards persistent antigen stimulation during infection and cancer [31]. The binding of PD1 to its ligand Programmed cell death ligand-1 (PD-L1) goes along with a suppressed T cell proliferation and cytokine secretion. For that reason, an increased expression of PD-L1 on tumor cells inhibits T cell induced immune surveillance. The administration of pembrolizumab and nivolumab prolongs survival of melanoma patients compared to chemotherapy or ipilimumab monotherapy [31]. The best results were achieved with the combination of ipilimumab and nivolumab [15, 32]. Despite an increased survival rate of metastatic melanoma patients after combination treatment 50 % of the patients do not benefit from long lasting effects [31, 33]. Therefore not only the identification and development of biomarkers to predict personal treatment response but also the investigation of resistance development mechanisms is necessary.

There are still many clinical trials ongoing to further investigate the role of potential targets for ICI in melanoma [31, 34]. Recently, lymphocyte activation gene-3 (LAG-3) was identified as an immune checkpoint molecule since it is expressed on activated T cells and binds major histocompatibility complex (MHC)II. Persistent antigen stimulation leads to an upregulated LAG3 expression on T cells, which induces tumor mediated T cell exhaustion and promotes the immunosuppressive role of regulatory T cells (Tregs). The use of relatlimab, a LAG3-blocking antibody, in combination with the PD1 inhibitor nivolumab showed improved PFS in melanoma patients compared to nivolumab monotherapy [35]. Other ICIs targeting T cell immunoglobulin and mucin-domain containing-3 (TIM-3) or T-cell immunoreceptor with immunoglobulin and ITIM domains (TIGIT) are still under investigation in clinical trials but extend the variety of promising therapeutic targets [34].

Adoptive cell therapy

T cells play a major role in regulating antitumor activity. The identification of tumor-infiltrating lymphocytes (TILs) and their capability to specifically recognize tumor cells led to the idea of adoptive cell therapy (ACT). The first successful attempt of ACT in metastatic melanoma patients using autologous TILs was performed in 1988 and convinced with an improved response rate compared to IL-2 monotherapy [36, 37]. TILs consist of $CD4^+$ and $CD8^+$ T cells, which can be isolated from the tumor and expanded *in vitro*. This is achieved by the digestion of resected tumor tissue in order to receive suspensions of single cells or small tumor fragments. The *in vitro* culture with IL-2 for two to three weeks leads to overgrowth and destruction of leftover tumor material by expanded lymphocytes. Pure cultures of lymphocytes can be used to investigate reactivity against the tumor in T cell cytotoxicity assays. Tumor reactive T cells are selected and further expanded in combination with anti-CD3 targeting the ϵ-subunit within the human CD3 complex and IL-2. It takes approximately six weeks to generate 10^{11} cells, which then can be infused into the patients after lymphodepletion [36, 38].

1.2 Melanoma-associated antigens

The effective function of ACT is based on the specificity of TILs to antigens, which are highly expressed in tumors. Antigens commonly expressed on melanoma cells can be divided into cancer germline antigens (CGAs), melanocyte differentiation antigens and neoantigens [31]. CGAs or cancer-testis antigens usually get silenced epigenetically after fetal development in adult tissue (besides germ cells and placental trophoblast). However, tumors often show an altered DNA

methylation pattern which leads to the ectopic expression of CGAs on melanoma cells like New York esophageal squamous cell carcinoma-1 (NYESO-1) or members of the melanoma-associated antigen (MAGE)-A family of proteins [39]. On the other hand, melanocyte differentiation antigens like Melanoma-associated antigen recognized by T cells (MART-1), Melan-A, glycoprotein 100 (gp100) and tyrosinase are involved in normal melanocyte differentiation. Therefore the expression of MART-1, gp100 and tyrosinase is not only limited to melanoma cells but instead they are also expressed by melanocytes. Another example for a surface protein that is highly expressed on melanoma cells is melanoma-associated chondroitin sulfate proteoglycan (MCSP), also known as CSPG4 or HMW-MAA, which is also prominent on other cancer entities including triple-negative breast cancer, head and neck squamous cell cancer and glioblastoma [40]. In contrast, neoantigens are tumor specific since they arise from somatic mutations which are absent in normal healthy tissue [31].

1.3 T cells

1.3.1 T cell development

The thymus is the primary lymphoid organ which supports the differentiation and selection of bone marrow (BM) derived lymphoid progenitors into mature naïve T cells. Its specialized three-dimensional (3D) organization composed of different cell types creates a complex unique environment for T cell development [41]. In humans, T cell generation in the thymus starts at day 60 of embryogenesis and is highly dependent on cellular interactions between the thymic stroma and the developing T cells (thymocytes) [42]. Thymic epithelial cells (TECs) constitute a key cell type of the thymic stroma by providing essential signals for T cell maturation and differentiation including positive and negative T cell selection [43].

BM derived $Lin^{-}CD34^{+}$ T lymphoid progenitors are attracted to the thymus by chemokines like C-C motif chemokine ligand 25 (CCL25) and C-X-C motif chemokine ligand 12 (CXCL12) secreted from cortical TECs and their interaction with the receptors C-C chemokine receptor type 9 (CCR9) and C-X-C motif chemokine receptor 4 (CXCR4), respectively. The expression of Notch ligands delta like canonical Notch ligand (DLL)1 and DLL4 on TECs in combination with adhesion molecules such as P-selectin promotes further induction of irreversible T cell lineage commitment [44–46]. Proliferation, survival and differentiation of the developing thymocytes are mediated by cytokines like IL-7 and stem cell factor (SCF) [47]. In the first stage of T cell development thymocytes do not express CD4 and CD8 and are for this reason defined as double negative (DN). The

DN stage can be divided into four substages (DN1-DN4) based on the expression of CD25 and CD44, DN1:$CD25^{-}CD44^{+}$; DN2:$CD25^{+}CD44^{+}$; DN3:$CD25^{+}CD44^{-}$ and DN4:$CD25^{-}CD44^{-}$ [48, 49]. During the DN3 stage, thymocytes start to express a pre-T cell receptor (TCR) as a result of a functional TCR β-chain rearrangement and a non-rearranged pre-Tα chain in a process called β-selection. A lack of pre-TCR complex expression at the DN3 stage leads to apoptotic death. Therefore, pre-TCR expression participates in the proliferation and differentiation of DN4 thymocytes. Via the immature single positive (ISP, $CD3^{-}CD4^{+}CD8^{-}$ in humans) stage thymocytes develop into $CD4^{+}CD8^{+}$ double positive (DP) cells. This transformation goes along with the TCRα gene rearrangement leading to TCRαβ complex expression on the cell surface of DP T cells [50]. Cells are now committed to the αβ-T-cell lineage [48, 49, 51, 52]. At that stage the functionality of the TCRαβ complex is tested via positive and negative selection of the DP T cells [50]. Immature DP T cells expressing a TCR with weak affinity to self-peptide-MHC complexes are induced to differentiate into immature $CD4^{+}$ or $CD8^{+}$ single positive (SP) T cells dependent on their specificity towards MHCI or MHCII [51, 53]. SP T cells showing no recognition of self-peptide-MHC complexes are selected for death by neglect. On the other hand, T cells that express TCRs with high affinity towards self-peptide MHC complexes are negatively selected and undergo apoptosis to induce T cell tolerance. This process which is also known as negative selection is carried out by TECs in the second compartment of the thymus, the medulla [53]. After selection, $CD4^{+}$ or $CD8^{+}$ SP T cells are able to leave the thymus via blood vessels [50].

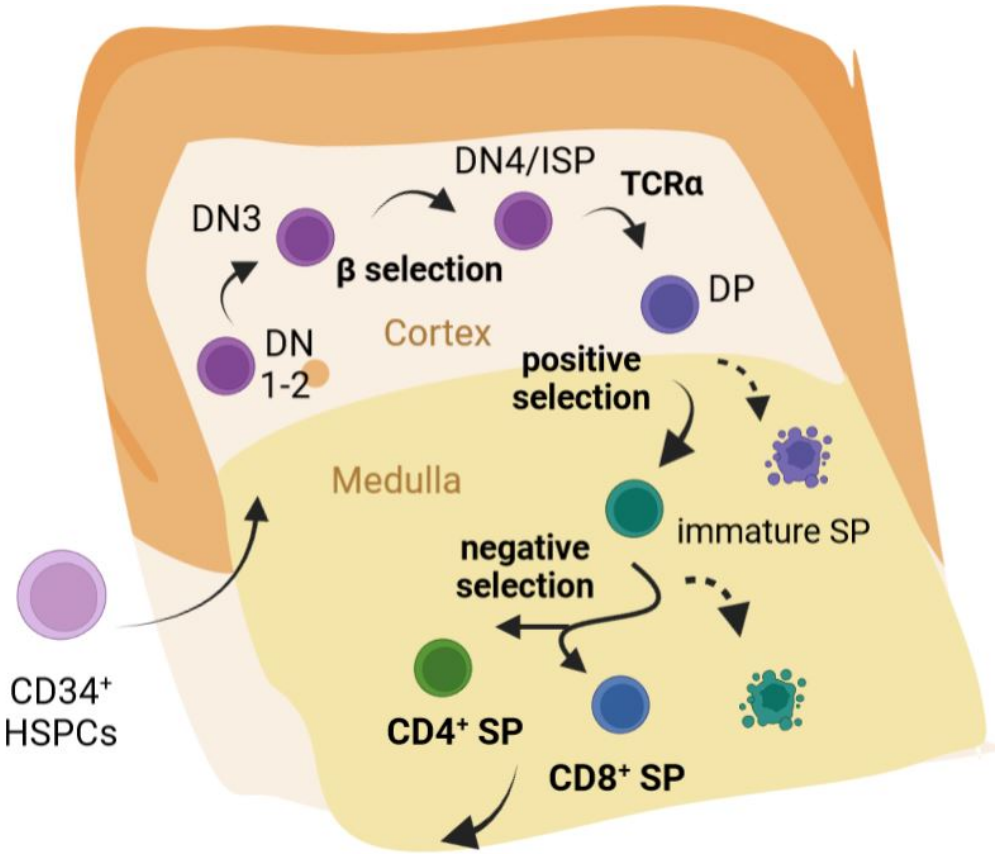

Fig. 1: T cell development in the human thymus. BM-derived $CD34^+$ T lymphoid progenitors enter the thymus via the medulla region. In the first stage thymocytes do not express CD4 and CD8 and are for this reason defined as double negative (DN). The DN stage can be divided into four substages (DN1-DN4) based on the expression of CD25 and CD44. During the DN3 stage, thymocytes start to express a pre-TCR in a process called β-selection. Via the immature single positive (ISP, $CD3^-CD4^+CD8^-$ in humans) stage thymocytes develop into CD4+CD8+ double positive (DP) cells. This transformation goes along with the TCRα gene rearrangement leading to TCRαβ complex expression on the cell surface of DP T cells. Functionality of the TCRαβ complex is tested via positive and negative selection of the DP T cells. Immature DP T cells expressing a TCR with weak affinity to self-peptide-MHC complexes are induced to differentiate into immature $CD4^+$ or $CD8^+$ single postitive (SP) T cells dependent on their specificity towards MHCI or MHCII. SP T cells showing no recognition of self-peptide-MHC complexes are selected for death by neglect. On the other hand, T cells that express TCRs with high affinity towards self-peptide-MHC complexes are negatively selected and undergo apoptosis to induce T cell tolerance. This process is known as negative selection. After selection, $CD4^+$ or $CD8^+$ SP T cells are able to leave the thymus via blood vessels. Figure adapted from Famili *et al.*, *Future Science OA* [50].

1.3.2 T cell generation *in vitro*

Major challenges of generating T cells *in vitro* are to recreate the complex architecture of the thymus in the form of an artificial niche, the diverse composition of the extracellular matrix (ECM) as well as the unique 3D organization of the thymic stroma. First approaches of reconstructing the thymic stroma were performed in 2D environment using TECs. The culture of TECs on feeder cells showed incomplete generation of lymphocyte progenitors and TECs finally lost the expression of important molecules for T cell development like Notch ligands, Forkhead box protein N1 (FOXN1) and MHCII [54–56]. The group of Zúñiga-Pflücker initiated the use of engineered OP9 cells for the differentiation of T cells from hematopoietic stem and progenitor cells (HSPCs) to circumvent these issues [57]. OP9 cells derived from mesenchymal stromal cells (MSCs) of the murine bone marrow of CSF1-deficient mice showed hematopoietic potential but were unable to induce further T cell differentiation [57, 58]. Instead the presence of DLL1 in combination with Fms-related tyrosine kinase 3 Ligand (FLT3-L) and IL-7 helped to support the generation of T cells from fetal liver progenitors and from umbilical cord blood via the consecutive intermediate stages of $CD7^+$ pro-T cells, $CD4^+$ intermediate SP, and $CD4^+CD8^+$ DP [57, 59]. Also the co-culture of human embryonic stem cells (ESCs) with DLL4-expressing OP9 cells supported T cell lineage commitment *in vitro* [60].

However, further T cell differentiation and maturation of TCR^+ $CD8^+$ SP T cells remained inefficient using the OP9 system with exception for umbilical cord blood (UCB)-derived HSPCs [61]. Presumably, the lack of the original 3D architecture of the thymus and the missing interaction between the thymic microenvironment including TECs, fibroblasts, endothelial and lymphatic cells as well as immune cells are the reasons for failed T cell lymphopoiesis *in vitro*. Similar to the *in vitro* TEC culture, the culture of Notch ligand-expressing OP9 stromal cell lines shows the drawback of lacking a 3D architecture [62]. For that reason, so called artificial thymic organoids (ATOs) developed by Seet *et al.* with ectopically expressing DLL4 murine stromal cells were created to simulate the 3D structure of the thymus. The recreation of human lymphopoiesis and therefore the generation of conventional naïve T cells from ESCs or pluripotent stem cells (PSCs) was possible using ATOs [63]. However, the use of genetically engineered murine stromal cell lines for the co-culture systems or ATOs causes difficulties in translating the system into clinical trials or further therapeutic applications.

1.4 Induced pluripotent stem cells

Induced pluripotent stem cells (iPSCs) were first reported in 2006 by Takahashi and Yamanaka. Originally generated from mouse embryonic fibroblasts (MEFs) and human skin fibroblasts by overexpression of the four transcription factors sex-determining region Y-box 2 (Sox2), Krüppel-like factor 4 (Klf4), octamer-binding transcription factor 4 (Oct4) and cMyc ("Yamanaka factors") iPSCs show similar characteristics in gene expression, proliferation, morphology and differentiation potential as ESCs [64, 65]. On the one hand they exhibit infinite proliferation capacity, on the other hand they have the ability to differentiate into all cell types of the three germ layers [66]. For that reason, iPSCs offer unique possibilities to study developmental biology, to model diseases, to discover and test new drugs and to find new innovative approaches in regenerative medicine.

1.4.1 Generation of iPSCs

For the reprogramming of somatic cells to iPSCs viral or non-viral methods are used either in combination with integrative or non-integrative transfer systems. Despite a very low reprogramming efficiency of less than 1 %, the Sendai-virus is a commonly used transfer system for human cells since it does not integrate into the host genome but replicates in the cytoplasm. Therefore, issues observed using integrative methods like the occurrence of insertional mutagenesis or tumorigenesis, inefficient silencing of the transgenes after iPSC formation or rather an eventual reactivation of transgenes are prevented [67–69]. In comparison, integrative viruses like retro- and lentiviruses which were initially used to generate iPSCs permanently integrate into the host genome and were therefore not suitable for prospective clinical applications [70]. Other non-integrative transfer systems include the adenovirus, the piggyBac system using transposons, minicircle vectors, episomal vectors, direct protein delivery and synthesized mRNA [71].

1.4.2 Current use of iPSCs in clinical applications

IPSCs can be generated from a variety of somatic cells like fibroblasts, keratinocytes, peripheral blood mononuclear cells (PBMCs) or urine cells but the differentiation of iPSCs to fully functional immune cells, neurons or cardiomyocytes is still challenging [72]. However, since the work with iPSCs is not associated with ethical concerns, clinical trials using the numerous possible applications of iPSCs are much easier to realize compared to the use of ESCs. Nevertheless, there are

only few iPSC-based therapies used as clinical applications since safety concerns like genetic instability, tumorigenicity, immunogenicity and heterogeneity of iPSCs as well as donor-specific human leukocyte antigen (HLA)-matching need to be overcome [73, 74]. The first clinical trial was already conducted 8 years after the discovery of iPSCs in 2014. Takahashi *et al.* described the successful transplantation of IPSC-derived retinal sheets into patients with retinal degeneration [73, 75]. Currently, iPSC-related clinical studies try to target different diseases worldwide e.g. ischemic cardiomyopathy, Parkinson's disease, graft-versus-host disease (GvHD) or spinal cord injuries [73]. Additionally, autologous iPSCs provide a source for *in vitro* drug testing and disease modeling in 3D arrangements like organoids and open up new possibilities for the recreation of more realistic models of human tissues [76].

1.5 DNA S/MAR vectors

The development of non-viral transfer systems for genome editing or supplementation purposes is of high interest for future gene and cell therapies. Effective gene delivery systems include non-integrative DNA scaffold/matrix attachment region (S/MAR) vectors, which offer persistent expression over hundreds of cell division by binding to the chromosomal scaffold during the mitotic interphase [77, 78]. As the name implies, the important part of the vector is the 60 to 5000 base pair (bp) long S/MAR element, which is originally derived from the human interferon β gene. S/MAR stands for scaffold/matrix attachment region and comprises AT-rich genomic DNA that enables the localization with transcription factors and the co-segregation with chromosomes during mitosis [79, 80]. In addition to the S/MAR site, an optimal S/MAR vector for gene expression purposes includes a promoter e.g. chicken beta-actin promoter (CAG) to ensure a stable expression of the gene of interest (GOI), selection marker or reporter genes and a poly A tail to stabilize the transcript. The vectors which were used in this study also include a bacterial origin of replication as well as an anti-repressiv Element40 (E40) which enhances the expression and improves stability of the vector. Since it was shown that S/MAR vectors were not epigenetically silenced and maintained episomal replication in a variety of different cell types they represent an effective gene delivery system which can be used for genetic modifications without impacting the genomic stability of the host cell [81, 82].

2 Research Objectives

Advanced metastatic melanoma is a devastating disease, which far too often ends fatal due to the limited choice of efficient therapeutic options. Adoptive T cell transfer holds great promise for the treatment of patients with advanced metastatic melanoma and is therefore subject of extensive research. The *in vitro* generation of patient-customized and antigen-specific T cells from hiPSCs could potentially provide clinicians with unlimited amounts of a high-potency tool to cure those patients who are today considered as terminally ill. However, there is still a need to improve this technique in order to make it applicable as standard for the use in clinical applications. For this reason, the aim of my thesis was to generate melanoma antigen-specific $CD8^+$ SP T cells from hiPSCs and to analyze their functionality in cytotoxicity assays and by FACS.

In detail, in the first part of this study I cloned the genes encoding a MART-1-specific TCR or a MCSP-specific CAR, respectively, into a S/MAR DNA vector backbone. Next, I transfected hiPSCs with these vectors and subjected them to a T cell differentiation process.

Since T cells derive from HSPCs, the first step of the differentiation process was to induce the hematopoietic specification of hiPSCs. For that, either the co-culture of hiPSCs on top of OP9 stromal cells or the formation of embryoid bodies was chosen. To differentiate the generated $CD34^+$ HSPCs to $CD4^+CD8^+$ DP T cells bioengineered OP9 stromal cells or a T cell Differentiation Kit (Stemcell Technologies) were used. The last step comprised the differentiation of $CD4^+CD8^+$ DP T to $CD8^+$ SP T cells by an extended activation.

Finally, the effector functions of the generated $CD8^+$ SP T cells were analyzed in cytotoxicty assays with melanoma cells lines.

All in all, five main objectives of this study were defined as followed:

1. Transfection of hiPSCs with S/MAR DNA vectors coding for melanoma antigen-specific TCR/CAR
2. Hematopoietic specification of the hiPSCs towards $CD34^+$ HSPCs
3. Differentiation of HSPCs into $CD4^+CD8^+$ DP T cells
4. Maturation of $CD4^+CD8^+$ DP T cells into $CD8^+$ SP T cells
5. Functional analysis of generated $CD8^+$ SP T cells

3 Materials and Methods

3.1 Materials

3.1.1 Reagents and Kits

Product	**Company**	**Catalog No.**
Adhesive clear qPCR seals	Biozyme	600238
Agarose NEEO Ultra Qualität	Carl Roth	2267.4
Ampicillin	Carl Roth	HP62.1
Biocoll/Ficoll	Sigma-Aldrich	L6715-500ML
CD3 MicroBeads, human	Miltenyi Biotech	130-050-101
DAPI	Roche	10236276001
DH5α competent cells	Thermo Fisher Scientific	18265017
EasySep Human CD34 Positive Selection Kit II	Stemcell Technologies	17856
Human IFN-γ ELISA Set	BD Biosciences	555142
Human TNF ELISA Set	BD Biosciences	555212
Endofree Plasmid Maxi Kit	Qiagen	12362
Foxp3/Transcription Factor Staining Buffer Set	Invitrogen	00-5523-00
Kanamycin	Carl Roth	T832
LB-Agar	Carl Roth	X965.3
LB-Medium	Carl Roth	X964.2
Live/Dead 700	BD Biosciences	564997
Midori Green Advance	Nippon Genetics	mg-04
NheI (10 U/L), FastDigest	Thermo Fisher Scientific	FD0974
Nuclease-free water	Carl Roth	T143.5
O'GeneRuler 1 kb DNA Ladder	Thermo Fisher Scientific	SM1163
O'GeneRuler 100bp DNA-Ladder	Thermo Fisher Scientific	SM1143
Paraformaldehyde	Sigma Aldrich	P6148-1KG
Platinum Taq Polymerase	Thermo Fisher Scientific	10966034
PVDF filter, 0.45 µm	Carl Roth	PP48.1
Qiaprep Spin Miniprep Kit	Qiagen	27106
Recombinant Human IFNγ	Peprotech	AF-300-32
RevertAid First strand cDNA Synthesis Kit	Thermo Fisher Scientific	K1622

Rnase-Free Dnase Set	Qiagen	79254
RNeasy Plus Mini Kit	Qiagen	74136
SOC Outgrowth Medium	New England BioLabs	B9020S
STEMdiff™ T Cell Kit	Stemcell Technologies	100-0194
SYBR Green PCR Master Mix	Applied Biosystems	4309155
T4 Ligase	Life Technologies	EL0011
Qiaprep Spin Miniprep Kit	Qiagen	12583
Venor Gem Classic Myco PCR Kit	Minerva Biolabs	11-1100
XhoI (10 U/L), FastDigest	Thermo Fisher Scientific	FD0694
X-treme GENE® 9 DNA Transfection Reagent	Roche Diagnostics	06365787001

3.1.2 Reagents for cell culture

Product	**Company**	**Catalog No.**
β-Mercaptoethanol	Gibco®Life Technologies	31350010
Bambanker freezing medium	Nippon genetics	BB02
Blasticidine	Sigma Aldrich	15205
Basic fibroblast growth factor (bFGF)	Peprotech	100-18B
Brefeldin A	Santa Cruz	sc-200861
Cell proliferation dye eFluor 450	Invitrogen	65-0842-85
Collagenase II	Gibco®Life Technologies	17101015
Collagenase IV	Gibco®Life Technologies	17104019
DMSO	Carl Roth	A994.2
DMEM, high glucose	Gibco®Life Technologies	41965-039
DMEM/F-12	Gibco®Life Technologies	11320033
Fetal Calf Serum (FCS)	Biochrom	S0115
Gelatine from porcine	Sigma-Aldrich	G2500-100G
HEPES	Gibco®Life Technologies	11560496
Ionomycin	Santa Cruz	sc-3592
Lipofectamine stem	Life Technologies	STEM00001
Matrigel	Corning	354277
Minimum Essential Medium α	Gibco®Life Technologies	32561037
Non-essential amino acids (NEAA)	Sigma-Aldrich	M7145
Normocin	InvivoGen	ant-nr-1

Opti-MEM®	Gibco® Life Technologies	31985062
PBS	Sigma-Aldrich	D8537
Penicillin/Streptomycin	Sigma-Aldrich	P4333
PMA	Santa Cruz	sc-3576
Polybrene Infection/Transfection Reagent	Sigma Aldrich	TR-1003-G
Recombinant human IL-7	Peprotech	200-07
ROCK inhibitor (Y27632)	Merck	SCM075
StemFit Basic 02 (A+B)	Nippon genetics	Basic02
STEMdiff Hematopoietic - EB Basal Medium	Stemcell Technologies	100-0171
STEMdiff Hematopoietic - EB Supplement A	Stemcell Technologies	100-0172
STEMdiff Hematopoietic - EB Supplement B	Stemcell Technologies	100-0173
StemPro Accutase	Gibco® Life Technologies	A1110501
StemSpan™ Lymphoid Differentiation Coating Material (100X)	Stemcell Technologies	09925
StemSpan Lymphoid Progenitor Expansion Supplement (10X)	Stemcell Technologies	09915
StemSpan T Cell Progenitor Maturation Supplement (10X)	Stemcell Technologies	09930
StemSpan SFEM II	Stemcell Technologies	09605
Trypan blue solution	Sigma-Aldrich	T8154
TrypLE Express	Thermo Fisher	12604-013
Trypsin-EDTA	Sigma-Aldrich	T3924

3.1.3 Cell lines

Cell line	**Source**	**Cell type**	**Mutation**
C32	ATCC	human melanoma cell line	BRAF V600E
HEK293T	ATCC	human embryonic kidney cells	wild type (WT)
hiPSC (HD11)	reprogrammed from patient fibroblasts with Sendai2.0	iPSCs	WT

HT144	ATCC	human melanoma cell line	BRAF V600E
OP9	provided by Pierre Guermonprez Centre national de la recherche scientifique (CNRS), Paris	murine stromal cell line	WT
OP9-FS12	provided by Pierre Guermonprez CNRS, Paris	murine stromal cell line expressing FLT3-L, SCF, CXCL12	expression of FLT3-L, SCF, CXCL12
WM266-4	ATCC	human melanoma cell line	BRAF V600D

3.1.4 Plasmids

Name	**Source**
p17-pSMARt-Ele40-CAG (S/MAR)	Richard Harbottle (DNA vector lab, DKFZ)
pCMV-dR8.91 (Packaging)	Konrad Hochedlinger (Harvard, Boston)
pCMV-VSV-G (Envelope)	Addgene No.8454
human DLL4	Andreas Fischer (DKFZ)
human MART-1 TCR	Michael Nishimura
human MCSP CAR	Niels Schaft (Universitätsklinikum Erlangen)
mCherry P2A	Daniel Novak (DKFZ)

3.1.5 Human primers

Target	**Forward Sequence**	**Reverse Sequence**
18S	GAGGATGAGGTGGAACGTGT	TCTTCAGTCGCTCCAGGTCT
CD34	CTACAACACCTAGTACCCTTGGA	GGTGAACACTGTGCTGATTACA
GATA3	GCCCCTCATTAAGCCCAAG	TTGTGGTGGTCTGACAGTTCG
LEF1	AGAACACCCCGATGACGGA	GGCATCATTATGTACCCGGAAT
NANOG	CAGTCTGGACACTGGCTGAA	CTCGCTGATTAGGCTCCAAC
NOTCH1	GAGGCGTGGCAGACTATGC	CTTGTACTCCGTCAGCGTGA

OKT4	GCTTGGGCTCGAGAAGGATGTGG	GGCCCTGGGGCCAGAGGAAA
RAG1	CTGTTCCGGGTGAGATCCTTT	TAACAATGGCTGAGTTGGGAC
SOX2	GCGTACCGGGTTTTCTCCATGCT	GTGAGGGCCGGACAGCGAAC
TCF7	CTGGCTTCTACTCCCTGACCT	ACCAGAACCTAGCATCAAGGA

3.1.6 Media and Buffers

Name	**Composition**
$CD8^+$ SP T cell maturation medium	T cell progenitor maturation medium 10 ng/mL IL-15 25 µl human CD3/CD28/CD2 cell activator
Cell freezing medium	80 % FCS 20 % DMSO mixed 1:2 with MEF medium
EB formation medium	EB medium A ROCK inhibitor (1:1000)
EB medium A	EB basal medium EB supplement A (1:200)
EB medium B	EB basal medium EB supplement B (1:10)
FACS buffer	PBS 2 % FCS 1 % EDTA
MACS buffer	PBS 0.5 % BSA 2 mM EDTA
Lymphoid pogenitor expansion medium	StemSpan SFEM II Expansion supplement (1:10)
StemFit complete medium	StemFit Basic 02 100 ng/mL bFGF Normocin (1:1000)
MEF medium	DMEM+GlutaMAXX 10 % FCS 1 % pen/strep 1 % NEAA

	0.1 mM β-Mercaptoethanol
OP9 medium	α MEM 10 % FCS 1 % pen/strep 1 % NEAA 0.1 mM β-Mercaptoethanol
T cell progenitor maturation medium	StemSpan™ SFEM II Maturation supplement (1:10)
T cell medium	RPMI 1640 10 % pen/strep 10 % FCS

3.1.7 Antibodies

Antibody	**Species**	**Company**	**Reference**	**Dilution**
CD3, BV785	human	Biolegend	317329	1:50
CD4, APC-Cy7	human	Biolegend	344615	1:50
CD8a, BV711	human	Biolegend	301043	1:50
CD25, PE-Cy7	human	Biolegend	302611	1:50
CD34, APC	human	Biolegend	343509	1:50
CD45, APC	human	Biolegend	304011	1:50
CD69, FITC	human	Biolegend	310904	1:50
CD107a, PE-Cy5	human	BD Biosciences	560947	1:50
DLL4, APC	human	R&D	FAB1506A	1:50
H-2Kk, FITC	mouse	Biolegend	116304	1:100
IFNγ, BV421	human	Biolegend	502531	1:50
MCSP, PE-Cy7	human	Biolegend	B283985	1:50
TCRα/β, BV421	human	Biolegend	306721	1:50
CD3 monoclonal (OKT3)	human	Thermo Fisher	16-0037-81	1 µg/ml
CD28 unlabeled	human	Beckman Coulter	IM1376	2 µg/ml

3.1.8 Equipment

Product	**Company**
15 ml and 50 ml Tubes	Falcon
6-well, 24-well plates	Greiner Bio-One
6-well, 24-well non-tissue culture-treated plates	Greiner Bio-One
5, 10, 25 ml Pipettes	Corning
96-well U-bottom Plate	Greiner Bio-One
ABI 7500 Real-Time PCR Machine	Applied Biosystems
AggreWell 400 plate	Stemcell Technologies
BD FACS Aria I and II	Biosciences
BD FACS Fortessa	BD Biosciences
CELLSTAR® Cell Culture Flask	Greiner Bio-One
Cell strainer, 40 µm	Carl Roth
Centrifuge 5810 R	Eppendorf
ChemiDoc™ Touch Imaging System	Bio-Rad
Cryotubes, 1.8 ml external thread	Thermo Fisher Scientific
EasySep Magnet	Stemcell Technologies
FACS Tubes	NeoLab
Hemocytometry	Neubauer
Leica DM LS light microscope	Leica
LS Column	Miltenyi Biotec
LSR Fortessa HTS	BD Biosciences
MACS MultiStand	Miltenyi Biotec
MicroAmp Optical 96 Well Plate qPCR	Thermo Fisher Scientific
Microplates 96 Well	Falcon
MidiMACS Separator	Miltenyi Biotec
Nanodrop Spectophotometer ND-1000	Peqlab Biotechnologie GmbH
Nikon Eclipse Ti Fluorescence Microscope	Nikon
Parafilm	
Rotilabo®-syringe filters, 0,22 µm	Carl Roth
Rotilabo®-syringe filters, 0,45 µm	Carl Roth
Table Centrifuge 5418 R	Eppendorf
Tecan Infinite F200 PRO	Tecan
Thermomixer compact	Eppendorf

3.1.9 Software tools

Name	Source
7500 Software v2.0.5	Applied Biosystems
ApE	M. Wayne Davis (Open Source)
BD FACSDiva	BD Biosciences
EndNote	Clarivate Analytics
FlowJo 7.2.2	FlowJo
GraphPad PRISM	GraphPad software
Image Lab™ Software 6.0.1	BioRad
Microsoft Office 2019	Microsoft
NIS-Element	Nikon
TeXstudio 4.2.3	https://texstudio.org

3.2 Methods

3.2.1 Cell culture

HiPSCs were cultured in StemFit complete medium (Nippon genetics) supplemented with 100 ng/mL basic fibroblast growth factor (bFGF) (Peprotech) and 1:1000 normocin (InvivoGen) on matrigel (Corning) coated 6-well plates. For coating, matrigel was thawed overnight at 4°C on ice and aliquoted according to manufacturer´s protocol based on the protein concentration. Aliquots were stored at -20°C and resuspended in 24 ml Dulbeccos's Modified Eagle Medium (DMEM)/F-12 medium (Gibco ®Life Technologies) directly before use. 6-well plates were incubated with 1 ml of matrigel/DMEM/F-12 mix for 1 h at 37°C. After incubation plates were either use immediately or sealed with parafilm and kept for up to two weeks at 4°C. Before reaching 100 % confluency, hiPSCs were passaged to fresh Matrigel-coated plates using StemPro Accutase (Gibco ®Life Technologies) and kept in complete StemFit medium with 1:1000 Rho-associated protein kinase (ROCK) inhibitor for the first 24 h. Medium change was performed every other/second day. For long time storage hiPSCs were frozen in Bambanker freezing medium (Nippon genetics) and stored at -80°C or in liquid nitrogen.

Human melanoma cell lines were cultured in DMEM (Gibco®Life Technologies) containing 10 % heat inactivated fetal calf serum (FCS) (Biochrom), 1 % penicillin/streptomycin (pen/strep) (Sigma-

Aldrich), 1 % non-essential amino acids (NEAA) (Sigma-Aldrich), and 0.1 mM β-mercaptoethanol (Gibco ®Life Technologies).

Murine OP9 stromal cell lines were maintained in αMinimum Essential Medium (MEM) (Gibco®Life Technologies) containing 20 % FCS, 1 % pen/strep (Sigma-Aldrich) and 0.1 mM β-mercaptoethanol (Gibco®Life Technologies) in gelatine (0.1 %, Sigma-Aldrich) coated flasks. Cultures were passaged just before they reached confluency. Co-cultures of OP9 cells with hiPSCs were maintained in OP9 differentiation medium in other words αMEM supplemented as above, except that 20 % FCS was replaced with 10 % FCS. For further T cell differentiation, co-cultures were supplemented with recombinant IL-7 as described in subsection 3.2.11.

All cells were stored at 37°C, 5 % CO2, and 95 % humidity. Mycoplasma tests were performed on regular basis using Venor GeM Classic Mycoplasma detection kit (Minerva Biolabs).

3.2.2 RNA isolation

Total ribonucleic acid (RNA) isolation was performed using RNeasy Mini Kit (Qiagen), according to manufacturer's instructions. Briefly, cell pellets were lysed with cell lysis buffer followed by lysate transfer to a column and three times washing with washing buffer. To avoid genomic DNA contamination on-column DNase digest was performed using RNase-free DNase (Qiagen) for 15 min at room temperature (RT). Elution of column-bound RNA was achieved using RNase-free water. RNA quality and quantity were determined with a NanoDrop ND-1000 spectrophotometer (PEQLAB Biotechnologie GmbH). RNA was stored at -80°C until use.

3.2.3 cDNA synthesis

Complementary DNA (cDNA) synthesis was performed from 500 ng of total RNA using the Revert Aid First Strand cDNA synthesis kit (Thermo Fisher Scientific), according to manufacturer's instructions. Generated cDNA was diluted 1:10 in nuclease-free water before performing real time quantitative PCR (qRT-PCR).

3.2.4 qRT-PCR

Messenger RNA (mRNA) expression levels were assessed using the ABI 7500 Real-Time polymerase chain reaction (PCR) System (Applied Biosystems) and the SYBR Green PCR master mix

(Thermo Fisher Scientific). Briefly, synthesized cDNA was combined with SYBR Green Master Mix and primers for the specific amplification of the mRNA of interest. For all experiments, 18S ribosomal RNA expression was used as an endogenous control. Finally, gene expression was calculated using the delta-delta Ct method. For statistical analysis a total of at least 3 independent experiments was used.

3.2.5 Plasmid preparation

For bacterial transformation 100 µl of Stbl3 or DH5α competent Escherichia coli (E.coli) bacteria were thawn on ice and 100 ng of plasmid DNA 2-10 µl of interest were added. The mix was incubated on ice for 15 min, heat shocked for 3 min at 42°C and incubated on ice for 10 min again. 500 µl of super optimal broth with catabolite repression (SOC) medium was added and the mix incubated for 1 h at 37°C while shaking. Selection of resistant bacteria took place on lysogeny broth (LB) agar plates containing 100 µg/mL ampicillin or kanamycin, respectively. For that, 50 µl of bacteria were plated out and incubated over night at 37°C. The next day, colonies were picked and separately grown in 3 ml of LB medium containing ampicillin (1:1000) or kanamycin (1:1000) overnight at 37°C while shaking. The next day, bacteria were collected by centrifugation followed by DNA isolation using the Qiaprep Spin Miniprep Kit (Qiagen) according to manufacturer's instructions. Restriction enzyme digestion followed by gel electrophoresis was used to validate the plasmid's identity. Bacteria carrying the plasmid of interest were further expanded in 200 ml LB medium supplemented with ampicillin or kanamycin and the Endofree Plasmid Maxi Kit (Invitrogen) was used for plasmid DNA isolation according to manufacturer's instruction. Quality and quantity of isolated DNA were determined using the NanoDrop ND-1000 spectrophotometer.

3.2.6 Lentiviral particle production

For lentiviral particle production, HEK293T cells were seeded one day before transfection. When cells reached 70-80 % confluency, they were transfected with the lentiviral packaging constructs pCMV-dR8.91, pCMV-VSV-G as well as the plasmid of interest (human DLL4, Andreas Fischer, Deutsches Krebsforschungszentrum (DKFZ)) using the X-tremeGENE transfection reagent (Roche). 12 h post transduction, the supernatant was discarded and replaced with fresh target cell medium (in this case OP9 medium). 24, 36 and 48 h post transfection the supernatant containing lentiviral particles was collected and filtered through 0.45 µm polyvinylidene difluoride (PVDF) filter (Carl Roth). The collected supernatants were used for transduction immediately or stored at -80°C for future use.

3.2.7 Lentiviral transduction and antibiotic selection

For transduction, 2 ml of virus solution was added to the OP9 cells. To increase the transduction efficiency, 6 µg/ml polybrene (Sigma-Aldrich) was added. 24 h post transduction, cells were re-infected with 2 ml fresh virus solution without polybrene. 24 h later, cells were washed with Phosphate-buffered saline (PBS) three times and OP9 medium was added afterwards. To remove non-transduced cells 25 µg/l blasticidine (Sigma-Aldrich) was added to the medium for four to five days or until the non-transduced control cells were no longer alive. Lentivirus production, collection, storage, and transduction were performed in a biosafety level II laboratory.

3.2.8 S/MAR DNA vector preparation

S/MAR vector P17-pSMARt-Ele40-CAG was kindly provided by Dr Richard Harbottle (DNA vector Lab, DKFZ) and used as the backbone construct for further modifications with melanoma antigen-specific receptor genes. Briefly, digestion of P17-pSMARt-Ele40-CAG was performed using restriction enzymes NheI and XhoI for 2 h at 37°C, followed by enzyme heat inactivation for 20 min at 80°C. The 6841 bp DNA fragment containing the S/MAR site, was purified by agarose gel extraction. The TCR construct against MART-1 was kindly provided by Michael Nishimura. The CAR construct against MCSP was received from Niels Schaft (Universitätsklinikum Erlangen). Both constructs were amplified by PCR using Phusion polymerase. After amplification constructs were ligated with mCherry (mCherry P2A) reporter gene and with the S/MAR vector using T4 ligase. Ligation products were further used for transformation into DH5α competent bacteria (see subsection 3.2.5).

3.2.9 Transfection and sorting of hiPSCs with S/MAR vectors

One day prior to transfection, HD11 hiPSCs were seeded at a density of 5 x 10^4 cells per well in a matrigel coated 24-well plate in Stemfit complete medium + ROCK inhibitor. The next day, medium was changed to ROCK inhibitor-free medium and the transfection mix consisting of 25 µl Opti-MEM + 1 µl lipofectamin stem (Life technologies) was prepared. 500 ng vector DNA was diluted in 25 µl Opti-MEM and the mix was added to the diluted lipofectamin. Ten minutes later the mix was added to the cells (50 µl/well). Medium change was performed every other/second day as routinely done and cells were transferred to 6-well plates before reaching confluency. Transfection efficiency was determined by quantifying mCherry expression using fluorescence microscopy.

3.2.10 Fluorescence activated cell sorting of S/MAR vector transfected mCherry$^+$ cells

Six days post transfection mCherry$^+$ cells were fluorescence activated cell sorted for the first time using BD fluorescence-activated cell sorting (FACS) Aria I or II (BD Biosciences). Therefore cells were detached using Accutase and resupended in 200 µl PBS stained with 4′,6-diamidino-2-phenylindole (DAPI) (1:5000). MCherry$^+$ cells were directly sorted into matrigel coated 24-well plates (50000 cells/well) with Stemfit complete medium + ROCK inhibitor. 24 h post sorting medium was changed to Stemfit complete medium without ROCK inhibitor. Sorting was repeated at day 19, 35, 46, 53 and 59 post transfection to generate a stable mCherry-expressing cell line.

3.2.11 OP9 co-culture system with hiPSCs

HiPSCs were differentiated to CD34$^+$ HSPCs using OP9 stromal cells. Briefly, OP9 stromal cells were seeded onto 0.1 % gelatine-coated 6-well plates one day before use. The next day, hiPSC from one 6-well plate were dissociated using StemPro Accutase (Gibco®Life Technologies) and transferred to one confluent OP9 6-well plate with OP9 differentiation medium (see 3.1.6). Medium changes were performed at day 4 and day 7 by removing 1.5 ml of medium from each well and adding 2 ml of fresh OP9 differentiation medium. At day 9 supernatant and cells were collected. For this purpose, 1 ml collagenase IV solution (1 mg/ml) was added to the cells and incubated for 20 min at 37°C. After 20 min collagenase solution was collected and cells were incubated with 1 ml 0.05 % trypsin-Ethylenediaminetetraacetic acid (EDTA) per well. Afterwards cells were collected, centrifuged, resuspended in PBS and filtered through a 40 µm cell strainer. Obtained cell suspension was used for CD34$^+$ HSPC isolation by fluorescence activated cell sorting or immunomagnetic cell separation using the EasySep human CD34 positive selection kit II (Stemcell Technologies) in combination with the EasySep magnet (Stemcell Technologies, see 3.2.13).

Further differentiation towards the CD4$^+$CD8$^+$ DP stage was performed by seeding CD34$^+$ cells on confluent OP9-FS12 monolayers in OP9 differentiation medium supplemented with 5 ng/ml IL-7 (Peprotech) based on the protocol by Good *et. al.* [83]. Medium changes were performed every second day. Non-adherent cells were passaged every five to seven days by gently pipetting and filtering through 40 µm cell strainer and seeding onto fresh confluent OP9-FS12 monolayers. On day 44, non-adherent cells were harvested and prepared for flow cytometric analysis of T cell marker expression (see Table 11).

3.2.12 Generation of T cells using the STEMdiff T cell kit

For the generation of $CD8^+$ SP T cells from hiPSCs the STEMdiff T cell kit (Stemcell Technologies) was used according to manufacturer's instructions. Briefly, per well of a 6-well Aggrewell plate 3.5 x 10^6 hiPSCs were seeded in embryoid body (EB) formation medium and centrifuged to capture them in the microwells to form EBs. Half-medium changes were performed on day 2 (EB medium A) and day 3 (EB Medium B). On day 5 EBs were harvested by dislodgement from the microwells and subsequent collection on 40 µm cell strainers. Cells were transferred into non-tissue culture-treated 6-well plates by washing them from the flipped strainer with EB Medium B. Half-medium changes were performed at day 7 and day 10. On day 12, EBs were harvested and dissociated using collagenase II (2500 U/ml) and TrypLE Express (Thermo Fisher) for 20 min at 37°C. DMEM/F-12 + 15 mM 2-[4-(2-hydroxyethyl)piperazin-1-yl]ethanesulfonic acid (HEPES) (Gibco) was added to the cell suspension followed by centrifugation and resuspension in FACS Buffer. Subsequently, $CD34^+$ HSPCs were isolated by Magnetic EasySep human CD34 positive selection as described in subsubsection 3.2.13.2.

Isolated $CD34^+$ HSPCs were analyzed by flow cytometry (see Table 10) and further used for the following differentiation to T cells. For that, 24-well plates were coated with StemSpan Lymphoid Differentiation Coating Material for 2 h at RT. Plates were washed with PBS and 5 x 10^4 cells were added per well in 50 µl Lymphoid Progenitor Expansion Medium. Half-medium changes were performed at day 19 and 23. At day 26, cells were harvested and reseeded into freshly coated 24-well plates at a density of 0.5 - 1 x 10^5 cells/well in 500 µl T cell Progenitor maturation medium. Half-medium changes were performed at day 30, 33 and 36 before the cells were harvested on day 40 and used for flow cytometry analysis (see Table 11) or further differentiated to CD8+ SP T cells. Following $CD8^+$ SP differentiation, CD4+$^+$$CD8^+$ DP T cells were seeded into freshly coated 24-well plates at a density of 5 x 10^5 cells/well. $CD8^+$ SP T cell maturation medium was prepared from 500 µl T cell progenitor maturation medium supplemented with 10 ng/ml Il-15 and 6.25 µl ImmunoCult CD3/CD28/CD2 T cell activator (Stemcell Technologies). 500 µl of fresh $CD8^+$ SP T cell maturation medium (without activator) was added to the cells three days after seeding. Seven days after seeding (day 47 in total) cells were harvested and analyzed by flow cytometry (see Table 11) or used for further functional experiments.

3.2.13 Isolation of CD34$^+$ HSPCs

3.2.13.1 Fluorescence activated cell sorting (FACS) for CD34$^+$ HSPCs

Fluorescence activated cell sortings were performed with the help of the flow cytometry core facility at the DKFZ. For this, cells were resuspended in 100 µl FACS Buffer and the following antibodies were used in 1:50 dilution: CD34 APC (Biolegend), mH-2Kk FITC (Biolgend). Cells were incubated for 30 min at 4°C in the dark. After incubation cells were washed for 3 times with FACS buffer and DAPI (1:5000) was added 10 min before acquisition as viability stain. CD34$^+$FITC(GFP)$^-$ population was sorted into sterile collection tubes with OP9 differentiation medium using BD FACS Aria I or II (BD Biosciences) with 100 µm nozzles. After sorting, cells were used for further differentiation steps.

3.2.13.2 Magnetic EasySep human CD34 Positive selection

CD34$^+$ HSPCs positive selection was performed using the EasySep human CD34 Positive selection Kit II (Stemcell Technologies) according to manufacturer's instruction. Briefly, cells were resuspended in 0.2 ml FACS buffer and 20 µl of selection cocktail was added. Following a 10 min incubation step at RT 10 µl RapidSpheres were added to the sample and incubated for 5 min. The sample was topped up with 2.3 ml of FACS Buffer and placed into the magnet for 3 min. Next, the supernatant was discarded and the steps repeated once or twice. Last, cells were resuspended in medium and used for further differentiation steps or flow cytometric analysis.

3.2.14 Flow Cytometry

For flow cytometric analysis BD LSR Fortessa was used. Cells were stained with different staining panels according to the differentiation state. For this, cells were resuspended in 100 µl FACS buffer with the respective antibody mix. Cells were incubated for 30 min at 4°C in the dark. After incubation cells were washed 3 times with FACS buffer and DAPI (1:5000) was added 10 min before acquisition as viability stain.

Tab. 10: Antibody staining panel for the analysis of HSPCs

Laser	Filter	Specificity	Fluorochrome	Dilution
405 nm Violet	VL450/50	DAPI		1:5000
488 nm Blue	BL525/50	mH-2Kk, OP9	FITC (GFP)	1:100
561 nm Yellow	YG610/20	mCherry		
640 nm Red	RL670/30	CD34	APC	1:50

Tab. 11: Antibody staining panel for the analysis of T cell markers on differentiating cells

Laser	Filter	Specificity	Fluorochrome	Dilution
355 nm UV	UV-450/50	DAPI		1:5000
405 nm Violet	VL780/60	CD3	BV786	1:50
405 nm Violet	VL710/50	CD8	BV711	1:50
405 nm Violet	VL610/20	CD5	BV605	1:50
405 nm Violet	VL450/50	TCRα/β	BV421	1:20
488 nm Blue	BL525/50	mH-2Kk, OP9	FITC (GFP)	1:100
561 nm Yellow	YG780/60	CD7	PE-Cy7	1:50
561 nm Yellow	YG610/20	mCherry		
640 nm Red	RL780/60	CD4	APC-Cy7	1:50
640 nm Red	RL670/30	CD45	APC	1:50

Intracellular staining for IFN-γ was performed using the Foxp3/Transcription Factor Staining Buffer Set according to manufacturer's instructions. Briefly, cells were stained with the surface antibody cocktail containing Live/Dead 700 as viability stain (see Table 12). After 30 min incubation at 4°C cells were washed with FACS buffer and resuspended in 200 µl of IC Fixation Buffer for 30 min at RT. Next, cells were washed with 1x Permeabilization Buffer and IFN-γ antibody was added in 100 µl of Permeabilization buffer to the cells and incubated for 30 min at RT. After incubation cells were washed twice with 1X Permeabilization buffer and resuspended in FACS buffer for analysis.

Tab. 12: Antibody staining panel for the analysis of T cell activation markers on CD8+ SP T cells after PMA/iono stimulation

Laser	Filter	Specificity	Fluorochrome	Dilution
405 nm Violet	VL780/60	CD3	BV786	1:50
405 nm Violet	VL710/50	CD8	BV711	1:50
405 nm Violet	VL450/50	**IFN**γ	BV421	1:100
561 nm Yellow	YG660/20	CD107a	PE-Cy5	1:100
640 nm Red	RL780/60	CD4	APC-Cy7	1:50
640 nm Red	RL710/50	L/D 700	AF700	1:5000
640 nm Red	RL670/30	CD45	APC	1:50

3.2.15 Isolation of PBMCs from whole blood buffy coat

PBMCs were isolated from whole blood buffy coats of healthy donors (DRK Blutspendedienst, Mannheim) using density gradient centrifugation. Briefly, blood was diluted 1:1 with PBS and layered over 15 ml Biocoll/Ficoll (Sigma-Aldrich). After centrifugation at 400xg for 30 min at RT with low acceleration and no brake the PBMC-containing interphase was collected and washed with PBS. PBMCs were resuspended in MACS buffer and kept on ice for further applications.

3.2.16 Isolation of $CD3^+$ cells from PBMCs

$CD3^+$ cells were isolated from PBMCs using magnetic-activated cell sorting (MACS) (Miltenyi). Briefly, 4x 10^7 cells were resuspended in 320 µl MACS buffer and incubated with 80 µl CD3 beads (Miltenyi) for 15 min at 4°C. After washing, cells were resuspended in 500 µll MACS buffer. In the meantime, positive selection columns (LS, Miltenyi) were placed into an appropriate MACS separator and activated with 3 ml of MACS buffer. As soon as the last drop fell, the cell suspension was added to the column and the columns were washed three times with 3 ml of MACS buffer. After washing, the column was removed from the separator and placed on top of a collection tube. $CD3^+$ cells were flushed out by using the plunger and adding 3 ml of MACS buffer twice to the column. Obtained $CD3^+$ cells were counted with trypan blue solution (Sigma-Aldrich) and used for FACS analysis or T cell proliferation experiments.

3.2.17 T cell proliferation assay

To evaluate their proliferative capacity, T cells were stimulated with CD3 and CD28 for 96 h. Therefore, 96-well U-bottom plates were coated with 1 µg/ml CD3 monoclonal antibody (OKT3, Thermo Fisher Scientific) and 2 µg/ml CD28 unlabeled antibody (Beckman Coulter) in 100 µl PBS for 2 h at 37°C. After 2 h, remaining PBS was removed by turning the plate upside down. At the same time, generated T cells or $CD3^+$ T cells were labeled with 10 µM cell proliferation dye eFluor 450 (Invitrogen) for 20 min at RT in the dark. Afterwards, cells were washed with PBS and resuspended in complete medium for counting and seeding. 4 x 10^4 cells were seeded into each well of a 96-well plate. Additionally, melanoma cells or supernatant were added to some wells. T cell proliferation was assessed 4 days later by flow cytometry using BD LSR Fortessa. Cell supernatants were collected for the analysis of IFNγ and TNFα levels by ELISA.

3.2.18 T cell stimulation with PMA and ionomycin

To assess degranulation and cytokine production of differentiated T cells, cells were stimulated with 20 ng/ml phorbol myristate acetate (PMA) and 1 µg/ml of ionomycin 4 h before harvest. After 1 h 5 µg/ml brefeldin A was added to inhibit the protein transport. Unstimulated and stimulated cells were analyzed for surface expression of CD107a indicating granulation and intracellular expression of IFNγ by FACS (see Table 12).

3.2.19 T cell cytotoxicity assay with human melanoma cell lines

To test the cytotoxic capacity of the differentiated $CD8^+$ SP T cells they were co-cultured with melanoma cell lines C32 and WM-266-4 for 24 to 48 h. Briefly, melanoma cells were stained with 10 µM cell proliferation dye eFluor 450 (Invitrogen) for 20 min at RT in the dark. Afterwards cells were washed with PBS and resuspended in MEF medium for counting and seeding. 5 x 10^4 cells were seeded into each well of a 24-well plate and kept at 37°C, 5 % CO2, and 95 % humidity for 24 h. The next day, $CD8^+$ SP T cells were seeded on top of the melanoma cells in 1:5/10/20 ratios. After 24 to 48 h, cells were harvested using trypsin and stained with 2.5 µl propidium iodide (PI) (BD Biosciences) per sample. Cells were analyzed by flow cytometry within 1 h after staining.

3.2.20 ELISA

Secreted human IFN-γ levels in supernatants from activated T cells cultured alone or in the presence of melanoma cells/supernatants were measured by ELISA (Human IFN-γ ELISA, BD), according to manufacturer's instructions. Briefly, 100 µl of anti-Human IFN-γ monoclonal capture antibody were added to the wells, sealed and incubated overnight at 4°C. The next day, plates were washed with wash buffer 3 times and subsequently blocked with 200 µl Assay Diluent for 1 h at RT. Plates were washed again 3 times and 100 µl of cell supernatant was added to each well and incubated for 2 h. The supernatant was aspirated and the plate was washes 5 times before 100 µl of biotinylated anti-human IFN-γ monoclonal antibody + streptavidin-horseradish peroxidase conjugate was added and the sealed plate incubated for 1 h. The antibody was aspirated and the plate was washed 7 times with wash buffer before 100 µl substrate solution was added to each well. The plates were incubated for 30 min at RT in dark. After 30 min 50 µl stop solution was added to each well and absorbance was read at 450 nm. TNF-α levels were measured the same principle as described above by ELISA (Human TNF ELISA, BD) according to manufacturer's instructions.

3.2.21 HLA typing

HLA typing of hiPSCs and melanoma cells was performed at the DKMS Life Science Lab gGmbH (Dresden) using the high throughput method.

3.2.22 Statistics

Statistical evaluations were done using GraphPad Prism Version 5. Data are always represented as mean ± standard error of the mean (SEM) and statistical significance is indicated using p-values (*$p < 0.05$; **$p < 0.01$; ***$p < 0.001$). One-way analysis of variance (ANOVA) was used to compare between multiple conditions and data sets. For the comparison of two groups a two-tailed student's t test was performed.

4 Results

4.1 Generation of S/MAR vectors encoding TCRs against melanoma antigens

Episomal S/MAR vectors offer the possibility to achieve efficient and persistent expression of a GOI without affecting the genomic stability of the host cell. Moreover, they are not epigenetically silenced. For that reason S/MAR vectors were applied as delivery system for the transfection of hiPSCs with a TCR or a CAR in this study. The S/MAR vector P17-pSMARt-Ele40-CAG was kindly provided by Dr. Richard Harbottle (DNA vector Lab, DKFZ) and it was used as the backbone construct for further genetic modifications. Figure 2A shows the MART-1-TCR S/MAR vector encoding the α- and β-chain of the melanoma antigen recognized by T-cells 1 (MART-1) as GOI together with mCherry-P2A as a reporter gene for future selection processes. The MART-1 TCR sequence was cut from the MART-1 TCR plasmid, which was kindly provided by Michael Nishimura, and cloned into the S/MAR vector P17-pSMARt-Ele40-CAG. The successful integration of the GOI into the vector was achieved by digestion with the restriction enzyme XbaI. The digestion with XbaI generated two expected fragments with 7949 bp and 2531 bp (Figure 2C). Further validation of the vector was performed by Sanger Sequencing (LGC genomics). The second vector which was used in this study encodes a CAR directed against the melanoma-associated chondroitin sulfate proteoglycan (MCSP) (Figure 2B). The GOI consists of the single chain variable fragment (scFv), the hinge regions, an intracellular CD3 signaling domain together with a truncated CD28 as well as mCherry as the reporter gene. The sequence for the MCSP CAR was cut from the MCSP plasmid, which was kindly provided by Niels Schaft (Universitätsklinikum Erlangen), and cloned into the S/MAR vector P17-pSMARt-Ele40-CAG. Digestion with XbaI revealed the successful integration of the GOI into the vector as shown in the agarose gel picture (Figure 2D) and verified by Sanger Sequencing (LGC genomics). Both generated constructs were used for further experiments in this study and referred to as MART-1 or MCSP, respectively.

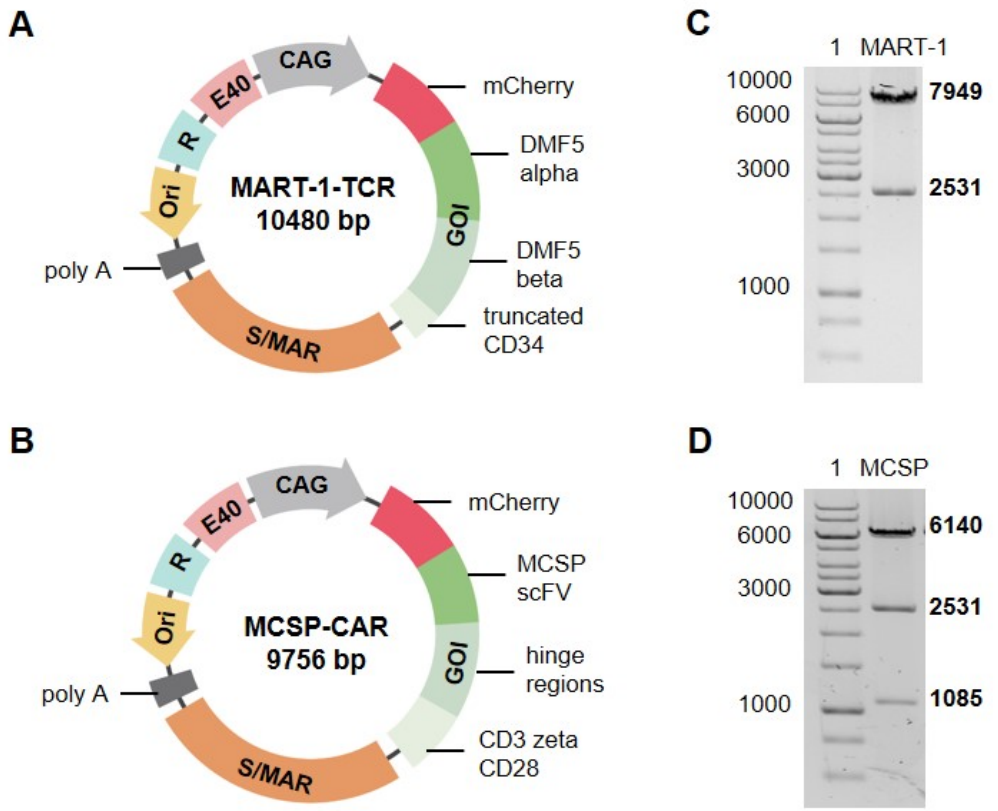

Fig. 2: S/MAR DNA vectors coding for a TCR/CAR specific for common melanoma antigens. Vector maps of S/MAR vector containing the S/MAR element (scaffold/matrix attachment region) for episomal replication and co-segregation during mitosis followed by a poly A tail for stabilization of the transcript. The origin of replication (Ori) enables replication in bacteria. For selection, a kanamycin resistance gene (R) is present. The anti-repressive Element40 (E40) enhances the expression and improves stability of the vector. As promoter CAG was chosen. The gene of interest (GOI) is expressed as a fusion protein between mCherry and the alpha and beta chain of the MART-1 TCR directed against MART-1 **(A)** or the CAR with single chain variable fragment (scFv) directed against MCSP, hinge regions as well as CD3 zeta and truncated CD28 **(B)**. Agarose gel picture of the MART-1-TCR vector **(C)** and MCSP-CAR **(D)** after digestion with the restriction enzyme XbaI. Bands show the size of the digested fragments.

4.2 Transfection of hiPSCs with S/MAR vectors against MART1 or MCSP

To generate T cells with a specificity against melanoma antigens, hiPSCs were transfected with the constructs mentioned in section 4.1 coding for the TCR against MART-1 or the CAR against MCSP, respectively. For the transfection of the hiPSCs Lipofectamine stem (Life technologies) was used. 1 day post transfection (dpt) transfection efficiency was examined by analyzing the expression of mCherry as reporter gene using fluorescence microscopy (Figure 3A). The expression of mCherry was clearly visible 1 dpt for both vectors. MCherry$^+$ cells were sorted at day 6 post transfection by FACS. The gating strategy for one representative sample is shown in Figure 3B. On average between 8 % and 33 % live cells were found to express mCherry 6 dpt. To establish a cell line with a stable expression of the receptors, cells were sorted at different time points post transfection. As shown in Figure 3C the percentage of mCherry$^+$ cells decreased enormously during the second sort to less than 1 %. During the third sort the percentage of mCherry$^+$ cells among live cells showed a high variety compared to the fourth sort, where 90-96 % mCherry$^+$ cells were detected. This percentage of mCherry$^+$ cells stayed stable for the upcoming 5th and 6th sorts (Figure 3C). The expression of mCherry was still detectable after repeated freezing and thawing cycles as shown in Figure 3D. In conclusion, the transfection of hiPSCs with S/MAR DNA vectors coding for melanoma antigen-specific receptors offers an efficient method for the generation of a stably expressing cell line. However, several rounds of FACS were necessary to remove cells without successful vector integration.

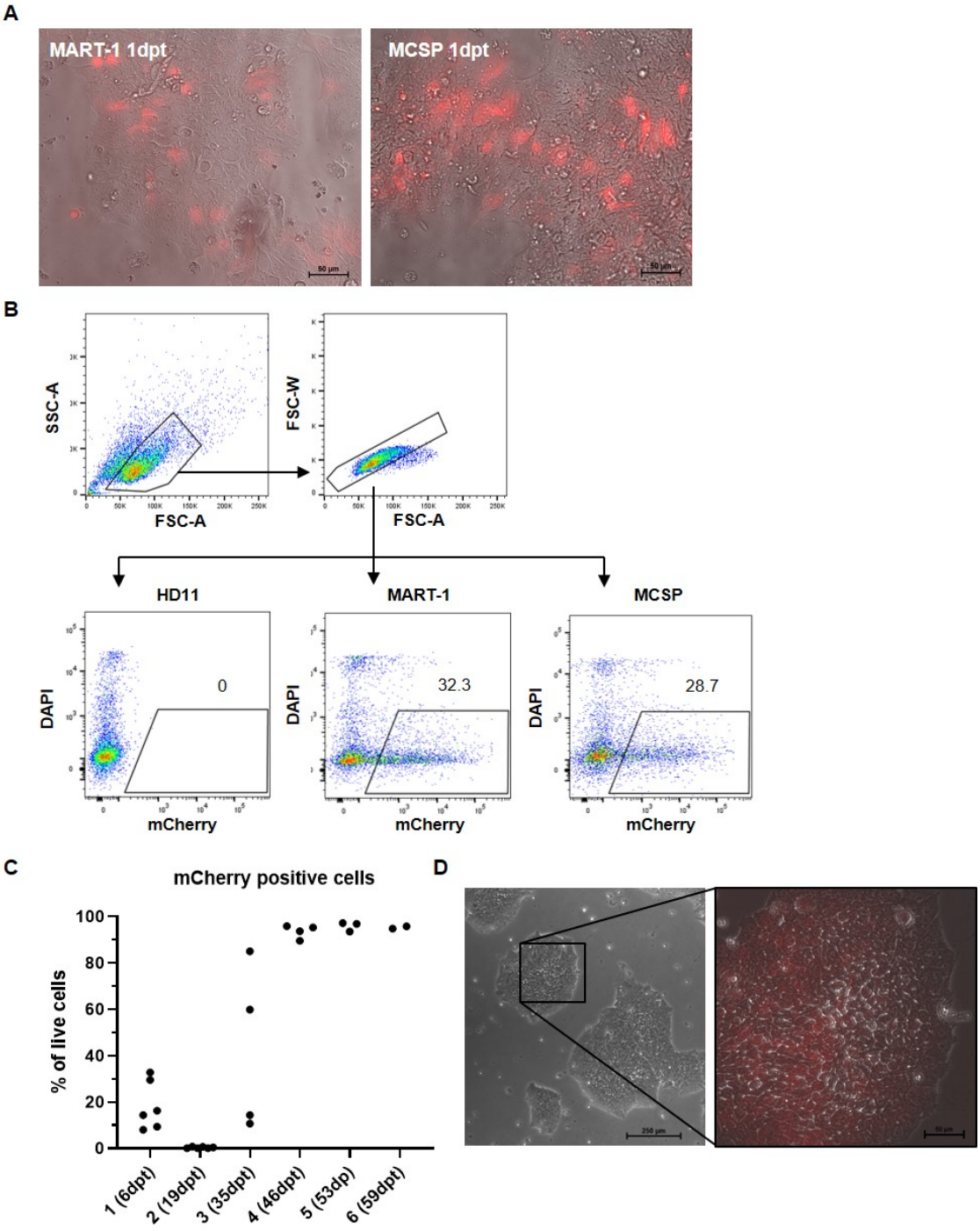

Fig. 3: Transfection of hiPSCs with S/MAR vectors coding for receptors directed against melanoma-associated antigens. A Fluorescent image of hiPSCs 1 day post transfection (dpt) with S/MAR vectors encoding mCherry-MART-1 or mCherry-MCSP, respectively. **B** Gating strategy for the isolation of mCherry$^+$ hiPSCs by FACS 6 dpt. Gates show the percentage of mCherry$^+$ live cells. **C** Percentage of mCherry$^+$ hiPSCs at different time points after transfection quantified by FACS. **D** Representative microscopic images of transfected hiPSCs transfected with MCSP-CAR after 5 rounds of FACS.

4.3 Transfection with S/MAR vectors did not alter the gene expression levels of the pluripotency genes NANOG and OCT4 in hiPSCs

To evaluate the influence of S/MAR vectors on the pluripotent character of hiPSCs, gene expression levels of the pluripotency-related genes NANOG, OCT4 and SOX2 in transfected (MART-1, MCSP) cells were quantified by RT-qPCR and further compared to untransfected (HD11) cells. As shown in Figure 4, there were only slight changes detected in the gene expression levels between the three cell lines. For NANOG and OCT4 slightly increased expression levels were seen in the transfected cells (MART-1, MCSP) compared to HD11. However, these alterations were not significant. On the other hand, SOX2 was significantly lower expressed in the transfected cells. Nevertheless, one can conclude that the use of S/MAR DNA vectors coding for a melanoma antigen-specific TCR/CAR did not alter the expression of pluripotency genes in hiPSCs to a relevant extent.

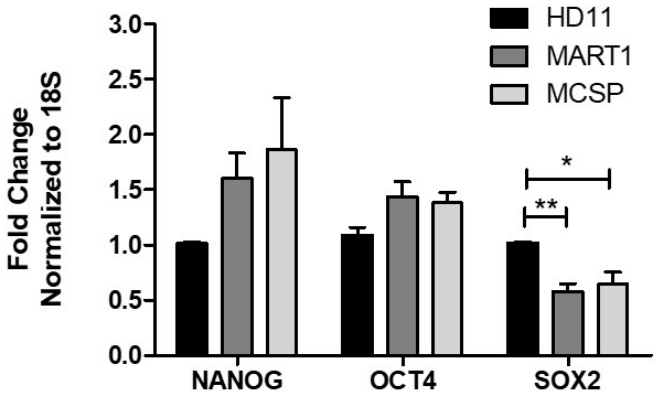

Fig. 4: Gene expression levels of pluripotency genes in hiPSCs before and after transfection with S/MAR vectors. Fold changes of mRNA expression levels of human pluripotency markers NANOG, OCT4 and SOX2 in untransfected (HD11) and with S/MAR vectors coding MART-1 TCR or MCSP-CAR transfected hiPSCs. 18S was used as endogenous control. Data represent mean ± SEM (n = 3). *p < 0.05; **p < 0.01.

4.4 Generation of CD34$^+$ HSPCs from hiPSCs using OP9 stromal cells

To induce the hematopoietic specification phase in order to facilitate the generation of CD34$^+$ HSPCs, hiPSCs were cultured on top of confluent GFP$^+$ murine BM-derived OP9 stromal cells (Figure 5A) for 9 days. The co-culture of hiPSCs (mCherry$^+$) on OP9 stromal cells (GFP$^+$) led to the appearance of cartwheel-like mesodermal structures after 9 days (Figure 5B). Following 9 days

of co-culture, CD34$^+$ HSPCs were isolated by FACS or CD34$^+$ EasySep immunomagnetic cell separation (STEMCELL Technologies) after enzymatic digestion with collagenase IV and trypsin.

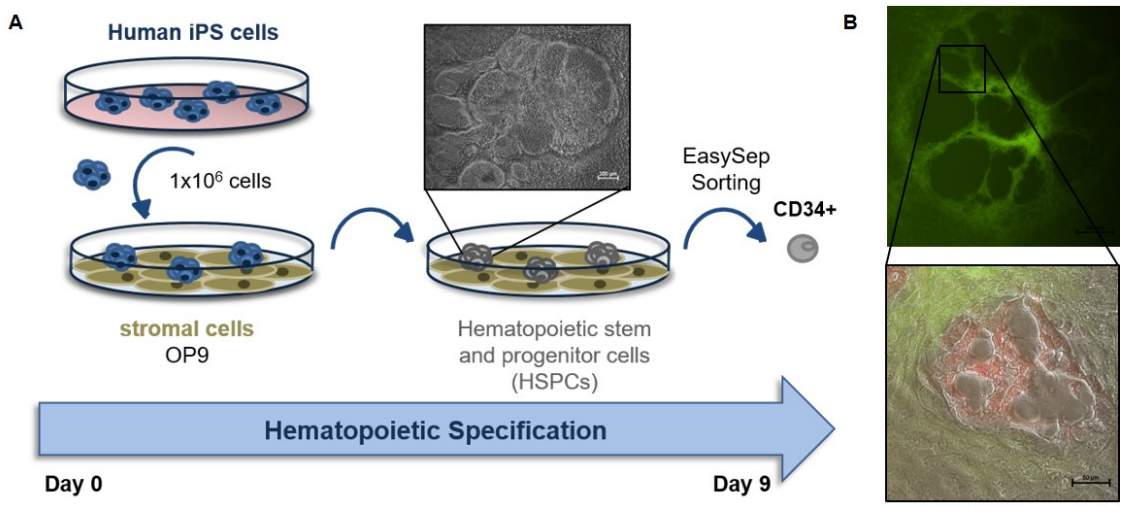

Fig. 5: Generation of CD34$^+$ HSPCs from hiPSCs using OP9 stromal cells. A Scheme of the hematopoietic specification procedure for hiPSCs towards CD34$^+$ hematopoietic stem and progenitor cells (HSPCs) by co-culture with GFP$^+$ OP9 stromal cells for 9 days. CD34$^+$ HSPCs were isolated by FACS or CD34$^+$ EasySep immunomagnetic cell separation at day 9 after enzymatic digestion with collagenase IV and trypsin. **B** Representative microscopy image showing the development of cartwheel-like mesodermal structures at day 9 of co-culture. Transfected hiPSCs expressing mCherry were surrounded by GFP$^+$ OP9 stromal cells.

The gating strategy for the isolation of CD34$^+$ cells by FACS is shown in Figure 6A as one representative example. The majority of cells of the co-culture system account for OP9 stromal cells which represent more than 90 % of all single cells. In general, about 10 % of the GFP$^-$ population expressed CD34$^+$ as a marker for the hematopoietic lineage. Compared to cell sorting, magnetic bead isolation of CD34$^+$ cells yielded a more diverse population. Figure 6B depicts a representative example for the analysis of CD34$^+$ cells among live cells isolated from the OP9 co-culture using magnetic beads. On average, the percentage of CD34$^+$ cells varied between 80 % for untransfected HD11 and 95 % for MART-1-transfected cells. For MCSP-transfected cells the percentage of CD34$^+$ cells was the lowest with 70 %. Additionally, mCherry expression was spotted in the majority of MART-1- (98 %) and MCSP-transfected (93 %) CD34$^+$ cells (Figure 6C). In conclusion, the 9 day co-culture of hiPSCs on OP9 stromal cells represents an appropriate method for the generation of CD34$^+$ HSPCs. Moreover, CD34$^+$ HSPCs can be isolated from the co-culture system by the use of FACS as well as immunomagnetic cell separation. However, a purer population of CD34$^+$mCherry$^+$ was obtained by using FACS.

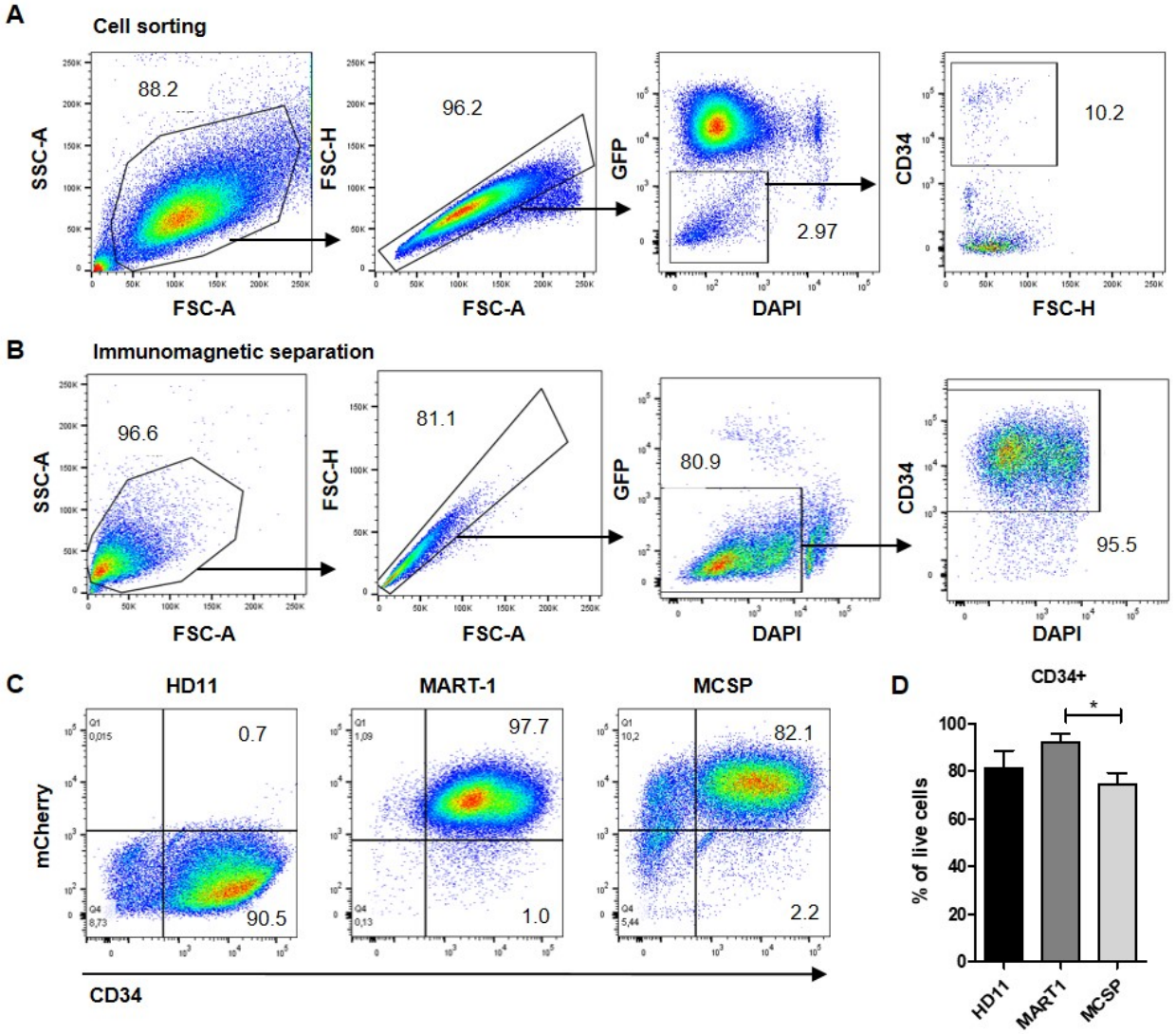

Fig. 6: Isolation of CD34$^+$ cells at day 9 of co-culture. **A** Representative gating strategy for FACS-based cell sorting of CD34$^+$ HSPCs. After gating on single cells and live cells, CD34$^+$ HSPCs were separated from GFP$^+$ stromal cells. **B** Representative FACS analysis of a CD34$^+$ HSPCs population isolated by immunomagnetic cell separation at day 9 of OP9 co-culture. **C** Representative dot plots showing the percentages of CD34$^+$ mCherry$^+$ cells after isolation using the Easy Sep magnet for untransduced HD11 cells and MART-1-transfected and MCSP-transfected HD11 cells. **D** Bar diagram showing the percentage of CD34$^+$ mCherry$^+$ cells isolated at day 9 from OP9 co-culture. Data represent mean ± SEM (n = 3). *p < 0.05.

4.5 Transfection with S/MAR vectors did not inhibit the gene expression of T cell-related differentiation genes

To evaluate the effect of the transfected TCRs on the expression of T cell-related differentiation genes, gene expression analysis of isolated $CD34^+$ cells was performed by RT-qPCR (Figure 7). No significant changes in the gene expression level of TCF7 between HD11, MART-1-transfected and MCSP-transfected $CD34^+$ cells were found. TCF7 encodes the transcription factor T cell factor-1 (TCF1), which regulates the β-selection of the pre-TCR complexes in DN3/4 thymocytes together with β-catenin and plays a role in the positive and negative selection of DP T cells [49]. Regarding the expression of GATA-binding protein 3 (GATA3), which acts together with Notch1 to commit thymic progenitors to the T-cell lineage, I saw a slight decrease in the expression level in MART-1-expressing $CD34^+$ cells compared to HD11 and MCSP-transfected cells [84]. The mRNA levels of recombination activation gene 1 (RAG1) which is expressed in immature lymphocytes and plays an important role in the generation of the antigen receptor repertoire did not differ between the samples [85]. In contrast, a significantly higher expression of lymphoid enhancer-binding factor 1 (LEF1), which is expressed in pre-T cells and acts together with TCF1 to promote β-selection was detected in MART-1-expressing cells [86]. A similar trend was noticed for the expression of NOTCH1 which is important for the development of $CD4^+CD8^+$ DP T cells in the thymus [55, 85]. Based on these results I assume that the expression of T cell-related differentiation genes is not suppressed in TCR/CAR-transfected cells during the differentiation process. Highest differences in the expression levels between the HD11 and MART1-transfected cells were found for LEF1 and NOTCH1. However for NOTCH1 I also saw a high variety in the expression levels between the different experimental replicates.

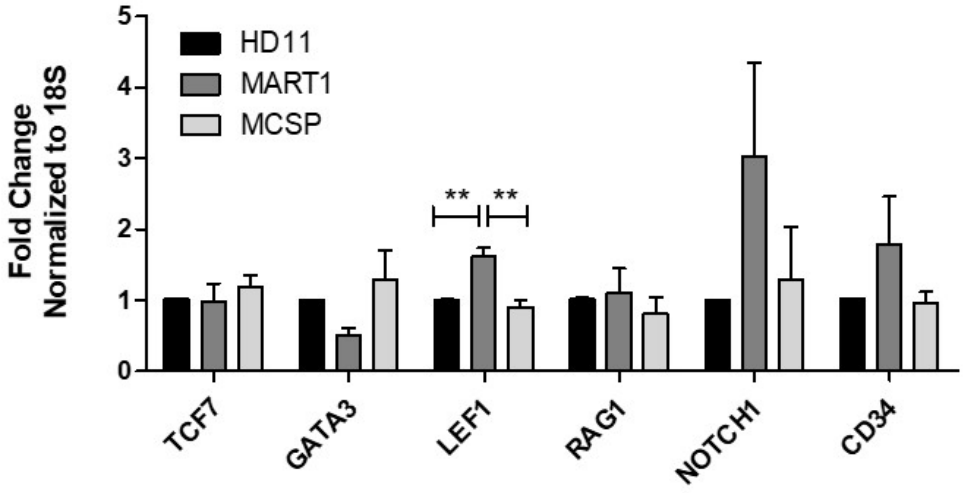

Fig. 7: Gene expression levels of T cell-related differentiations genes in CD34$^+$ HSPCs before and after transfection with S/MAR vectors. Fold changes of mRNA expression levels of T cell-related differentiation genes in untransfected (HD11) and transfected (MART-1, MCSP) CD34$^+$ cells. Data represent mean ± SEM (n = 3-4). **p < 0.01.

4.6 Bioengineering of OP9 cells to express the human Notch ligand DLL4

Important factors for the differentiation of HSPCs towards the lymphoid lineage include IL-7, FLT3-L, and CXCL12 as well as the NOTCH ligands DLL1 and DLL4. DLL4 which binds to the NOTCH receptor was shown to induce T cell differentiation of human cord blood and embryonic stem cells [59, 60]. For that reason, OP9 cells expressing FLT3-L, SCF and CXCL12 (OP9-FS12, kindly provided by Pierre Guermonprez, CNRS) were transduced with a lentiviral vector coding for human DLL4 (Figure 8A). Transduced OP9-FS12-hDLL4 cells were selected with 25 µg/ml blasticidine for 5 days. Figure 8B shows the DLL4 expression of GFP$^+$ transduced OP9-FS12hDLL4 cells compared to untransduced OP9-FS12 cells after selection. In detail, 75 % of the OP9-FS12hDLL4 cells were expressing DLL4 after selection. Therefore, they were further used as feeder cell line for the following T cell lineage differentiation of the HSPCs.

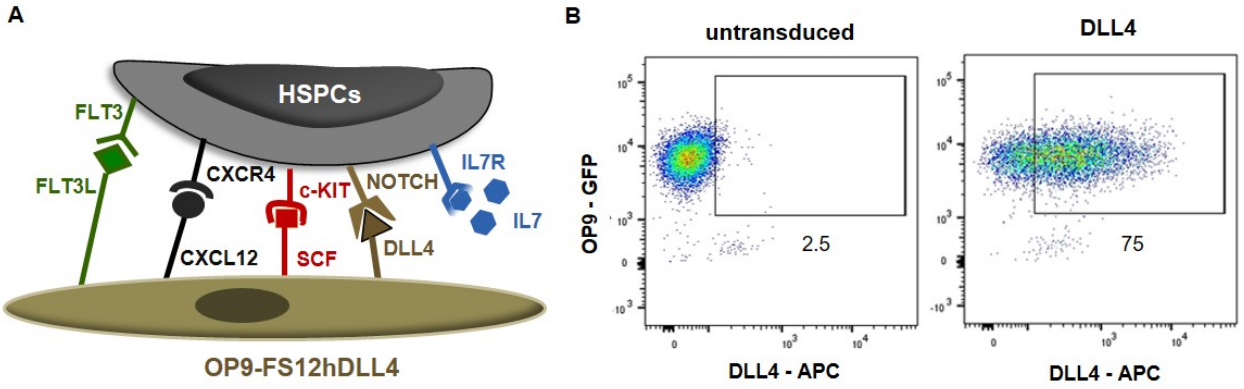

Fig. 8: Transduction of bioengineered OP9 stromal cells with a lentiviral construct coding for human DLL4. A Scheme of OP9 stromal cells expressing the important factors for T cell differentiation FLT3-L, SCF, CXCL12 and hDLL4 (OP9-FS12hDLL4) on their surface , which then interact with their receptors on the surface of HSPCs. **B** Representative dot plots of untransduced or hDLL4-transduced OP9-FS12 stained for the expression of hDLL4. Cells were gated on live cells. Numbers indicate the percentage of DLL4 expressing live cells.

4.7 *In vitro* replication of the T cell differentiation process using bioengineered OP9 cells

To further induce T cell differentiation isolated $CD34^+$ cells were seeded on top of confluent OP9-FS12hDLL4 cells in medium supplemented with IL-7 (Figure 9). After 35 days in co-culture, developing semiadherent cells were analyzed for T cell marker expression by FACS. The co-culture of $CD34^+$ cells on top of OP9-FS12hDLL4 cells supplemented with recombinant IL-7 induced T cell lineage commitment of $CD34^+$ HSPCs, as shown by the appearance of $CD45^+CD3^+TCR\alpha^+$ cells (Figure 10A). On average, the percentage of developing $CD4^+CD8^+$ DP T cells varied between 72 % and 89 % at day 44. In conclusion, the 2D co-culture of $CD34^+$ HSPCs on OP9-FS12hDLL4 cells in medium supplemented with recombinant IL-7 facilitated the differentiation of $CD4^+CD8^+$ DP T cells. However, the maturation of $CD8^+$ SP T cells remained insufficient using this OP9 co-culture system. In general, less than 10 % of the $CD3^+TCR\alpha\beta^+$ cells were identified as $CD8^+$ SP whereas the amount of $CD4^+CD8^+$ cells varied between 70 % and 90 % (Figure 10B).

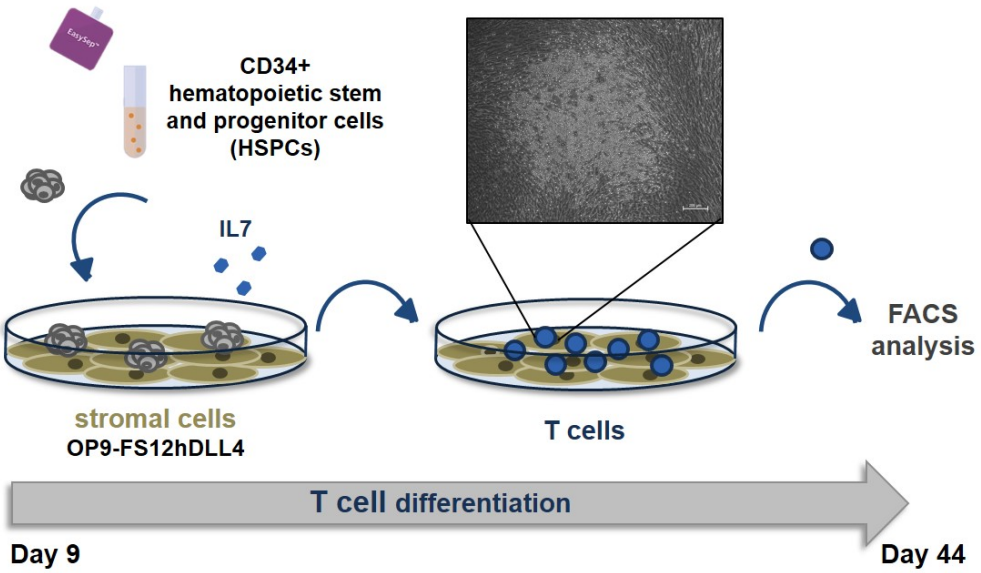

Fig. 9: Generation of CD4$^+$CD8$^+$ DP T cells from CD34$^+$ cells. Scheme of the differentiation process for the generation of CD4$^+$CD8$^+$ T cells using bioengineered OP9 cells. CD34$^+$ HSPCs were isolated from the days 9 OP9 co-culture system using immunomagnetic cell separation and seeded on top of confluent OP9-FS12hDLL4 cells in medium supplemented with recombinant IL-7. After additional 35 days in culture, semi-adherent cells were harvested and analyzed for the expression of T cell markers by FACS.

4.8 Feeder-free differentiation system: Generation of CD34$^+$ HSPCs in EBs

Differentiation methods using feeder based co-cultures for the *in vitro* generation of T cells are not suitable for subsequent applications due to the presence of feeder cells. For that reason, alternative assays without feeder cells offer better perspectives regarding the use in future cancer treatment strategies. The STEMdiff T Cell Kit (Stemcell Technologies) with serum-free media and supplements was used to generate CD34$^+$ HSPCs from hiPSCs in embryoid bodies (EBs) in Aggrewell plates (Figure 11A). After 12 days, EBs were harvested, digested with collagenase II and trypsin followed by CD34$^+$ HSPCs enrichment using EasySep positive selection. Figure 11B shows a representative FACS plot after CD34$^+$ selection of MART-1- and MCSP-transfected cells. The percentage of CD34$^+$ cells among live cells was found to be between 81.1 % (MART-1) and 77.9 % (MCSP). Additionally, more than 95 % of the cells were expressing the reporter gene mCherry. In summary, generating EBs using special Aggrewell plates in combination with serum-free medium and supplements supported hematopoietic specification without vector silencing similar to the 9 day co-culture on top of OP9 stromal cells.

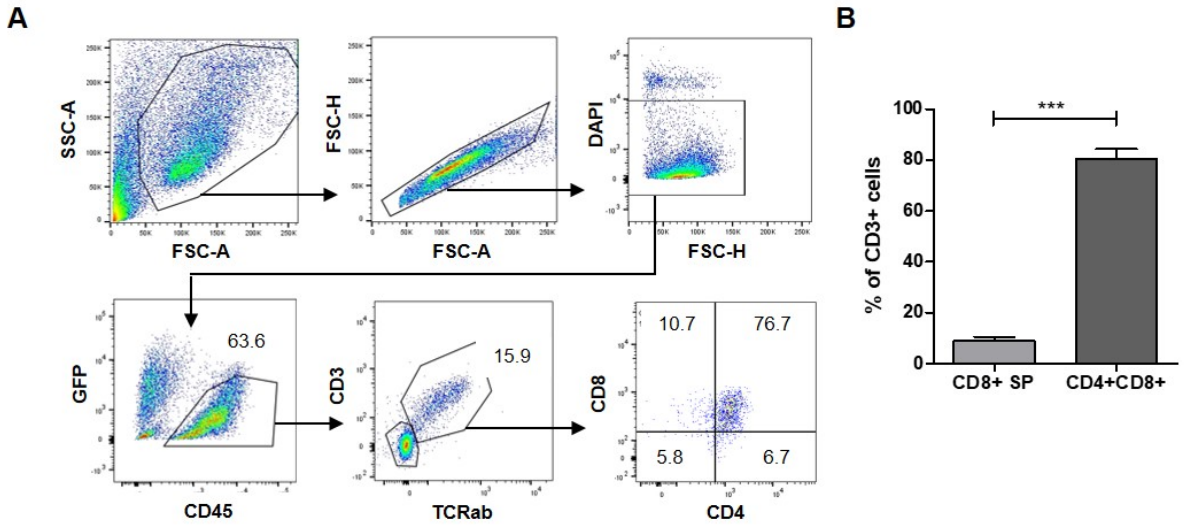

Fig. 10: Generation of CD4$^+$CD8$^+$ T cells using the bioengineered OP9 co-culture system. A Representative flow cytometry profile of differentiating cells at day 44 of co-culture. Cells were gated on live GFP-CD45$^+$ cells showing the expression of CD3, TCR$\alpha\beta^+$, CD4 and CD8. Cells were cultured on OP9-FS12hDLL4 in medium supplemented with recombinant IL-7. **B** Diagram showing the percentage of CD8$^+$ SP and CD4$^+$CD8$^+$ DP T cells from 4 independent experiments gated on CD3$^+$ cells. Data represent mean ± SEM (n = 4). ***p < 0.005.

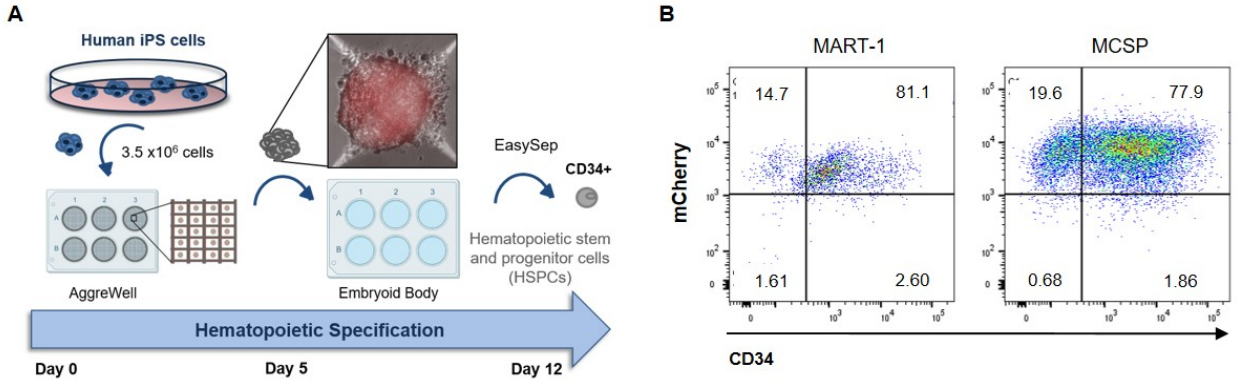

Fig. 11: Generation of CD34$^+$ HSPCs in EBs using Aggrewell plates. A Scheme of the differentiation process for the generation of CD34$^+$ HSPCs in embryoid bodies using Aggrewell plates and serum-free media $^+$ supplements. CD34$^+$ HSPCs were isolated after 12 days and enriched by immunomagnetic cell separation. **B** Representative FACS plot after CD34$^+$ selection of MART-1- and MCSP-transfected cells showing the expression of CD34 and mCherry. Cells were gated on live cells.

4.9 Feeder-free differentiation system: Generation of $CD4^+CD8^+$ DP T cells from $CD34^+$ HSPCs

Following the hematopoietic specification phase, T cell differentiation was induced by culturing $CD34^+$ HSPCs on lymphoid coating material in lymphoid progenitor medium for additional 28 days. After 14 days, the cells were passaged to freshly coated plates (Figure 12A). Figure 13 shows a representative FACS plot including gating strategy of developing T cells after 28 days of culture (total 40 days). Live cells were analyzed for the expression of T cell markers CD4 and CD8. 45 % of the MART-1 transfected cells were expressing CD4 and CD8 at day 40 of differentiation. For MCSP-transfected cells the percentage of $CD4^+CD8^+$ DP cells was much lower with about 1.8 %. Almost 100 % of the $CD4^+CD8^+$ population were expressing CD45 (for both MART-1- and MCSP-transfected cells), whereas only 18.9 % or 2.5 % were expressing CD3, respectively. For the small $CD8^+$ SP population a very low CD3 expression was found as well. Further analysis of total live cell population revealed a still existing mCherry expression for MART-1- and MCSP-transfected cells. However, the amount of $mCherry^+$ cells differed between 13.3 % for MART-1- and 84.6 % for MCSP-transfected cells.

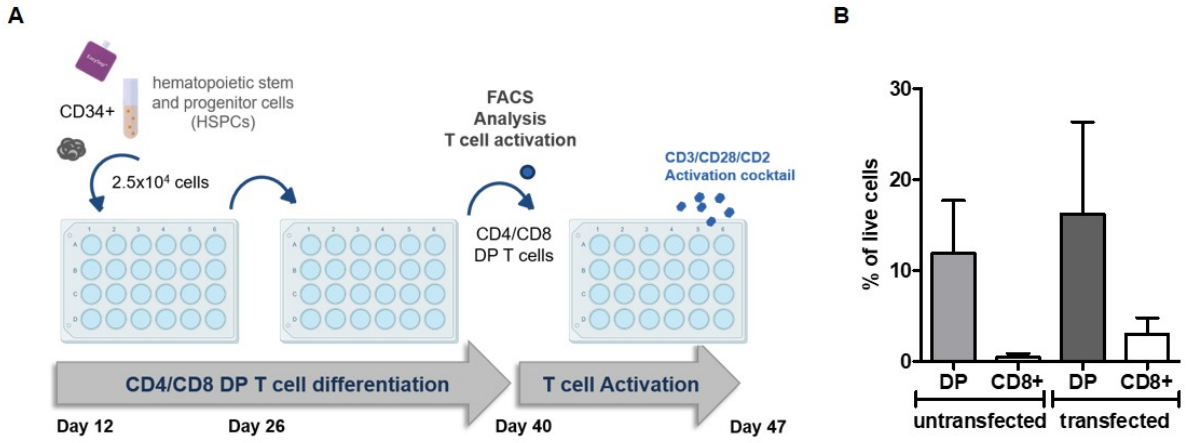

Fig. 12: Generation of $CD8^+$ T cells from $CD34^+$ cells. A Scheme of the differentiation process for the generation of $CD8^+$ T cells using lymphoid coating material in combination with lymphoid progenitor medium (Stemcell Technologies) for 28 days. At day 40 developing $CD4^+CD8^+$ DP T cells were analyzed for T cell marker expression by FACS or further activated with a cocktail containing CD3/CD28/CD2 and supplemented with IL-15. **B** Diagram showing the percentage of $CD4^+CD8^+$ DP and $CD8^+$ SP T cells at day 40 of differentiation gated on live cells. Data represent mean ± SEM (n = 2-4).

Taken together, the generation of $CD4^+CD8^+$ DP T cells from $CD34^+$ HSPCs using lymphoid

coating material and lymphoid progenitor medium for 28 days was successful. However, the efficiency rate of the differentiation varied a lot between different experiments, from 1 % and 45 % for the transfected cells and from 6 % up to 18 % for the untransfected cells (Figure 12B). MCherry expression was still detectable in MART-1- and MCSP-transfected cells after 40 days of differentiation with differences in the percentage of live cells. For MART1, 13.3 % of the total live population was expressing mCherry, whereas for MCSP 84.6 % of the cells were still expressing it. The persistent mCherry expression after 40 days of differentiation suggests a high efficacy of the S/MAR vectors.

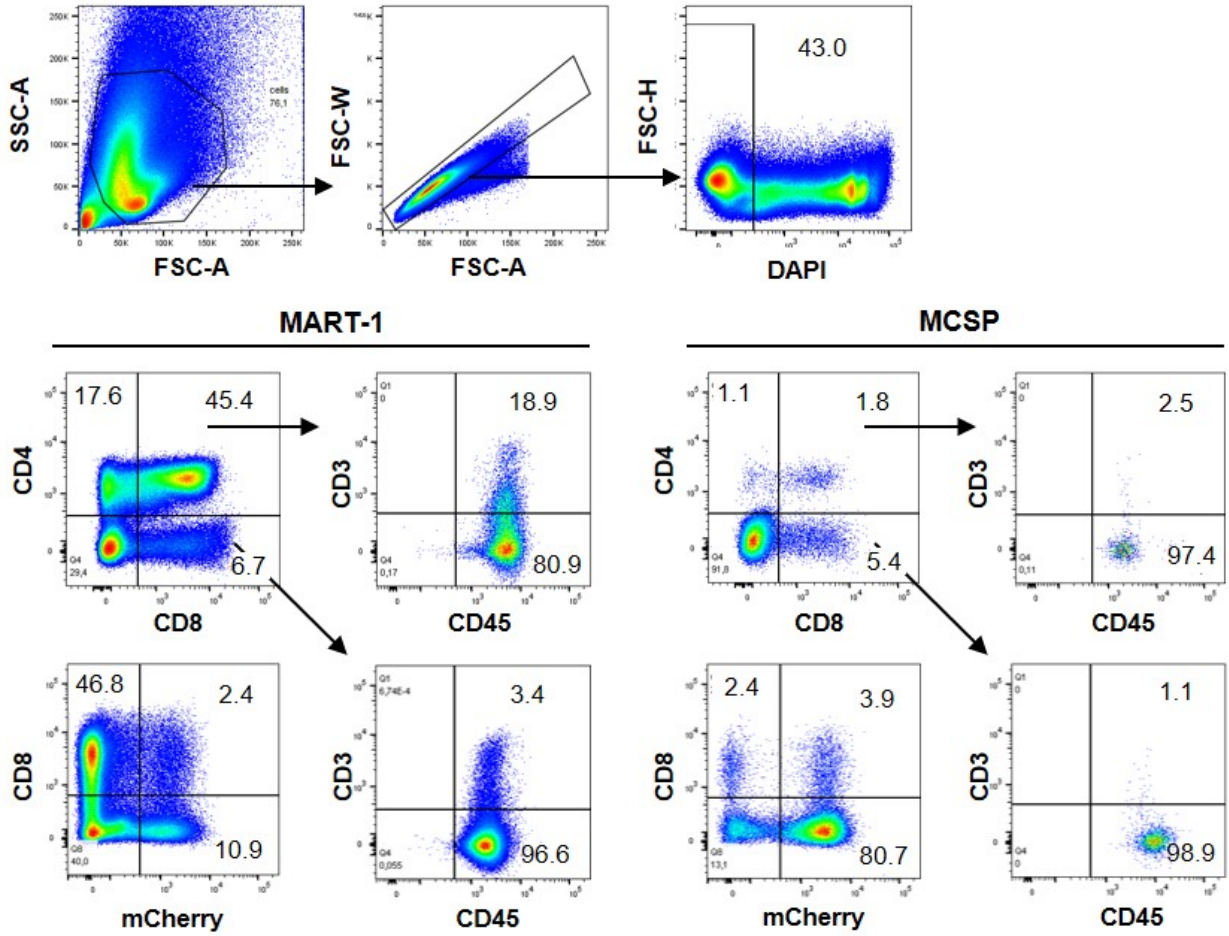

Fig. 13: Generation of CD4$^+$CD8$^+$ DP T cells from CD34$^+$ HSPCs. Representative flow cytometry profile of differentiating cells at day 40 showing the gating strategy for the identification of total live population and the expression of CD4, CD8 and mCherry in the live population for MART-1- and MCSP-transfected cells. CD4$^+$CD8$^+$ DP population and CD8$^+$ SP population were further analyzed for CD3 T cell marker and CD45 leukocyte marker expression. MCherry expression was quantified from total live cell population and analyzed together with CD8 expression.

4.10 $CD4^+CD8^+$ DP T cells derived from $CD34^+$ HSPCs did not show effector functions

$CD4^+CD8^+$ DP T cells at day 40 of differentiation were analyzed for their proliferative capacity and ability to secrete pro-inflammatory cytokines like IFN-γ and TNF-α upon CD3/CD28 stimulation for 96 h. As positive control human $CD3^+$ cells freshly isolated from healthy donor PBMCs were used. As shown in Figure 14A, CD3/CD28 stimulation induced the proliferation of CFSE-labeled $CD3^+$ T cells compared to unstimulated cells. However, CFSE-labeled $CD4^+CD8^+$ DP T cells did not show any increase in their proliferative capacity after stimulation. The addition of supernatants from HT144 and MeWo human melanoma cell lines did not increase the amount of proliferating $CD4^+CD8^+$ DP cells. In contrast, up to 93 % of the $CD3^+$ cells started to proliferate in response to melanoma cell supernatants (Figure 14A). To investigate the capacity to secrete the pro-inflammatory cytokines IFN-γ and TNF-α the supernatants of stimulated cells were analyzed by ELISA (Figure 14 B, C). Secreted IFN-γ and TNF-α could be detected in the supernatant from stimulated $CD3^+$ cells but not in the supernatant from $CD4^+CD8^+$ DP T cells. The co-culture with melanoma cell supernatant or melanoma cells led to a 10 - 150 fold increase in IFN-γ secretion and 10 - 15 fold increase in TNF-α secretion for $CD3^+$ cells. For $CD4^+CD8^+$ DP cells the stimulation did not have any effect on the secretion of pro-inflammatory cytokines. The observed results led to the assumption that differentiated T cells at the $CD4^+CD8^+$ DP stage did not yet acquire effector T cell functions and were therefore not able to respond to T cell-specific stimulation with proliferation or cytokine secretion.

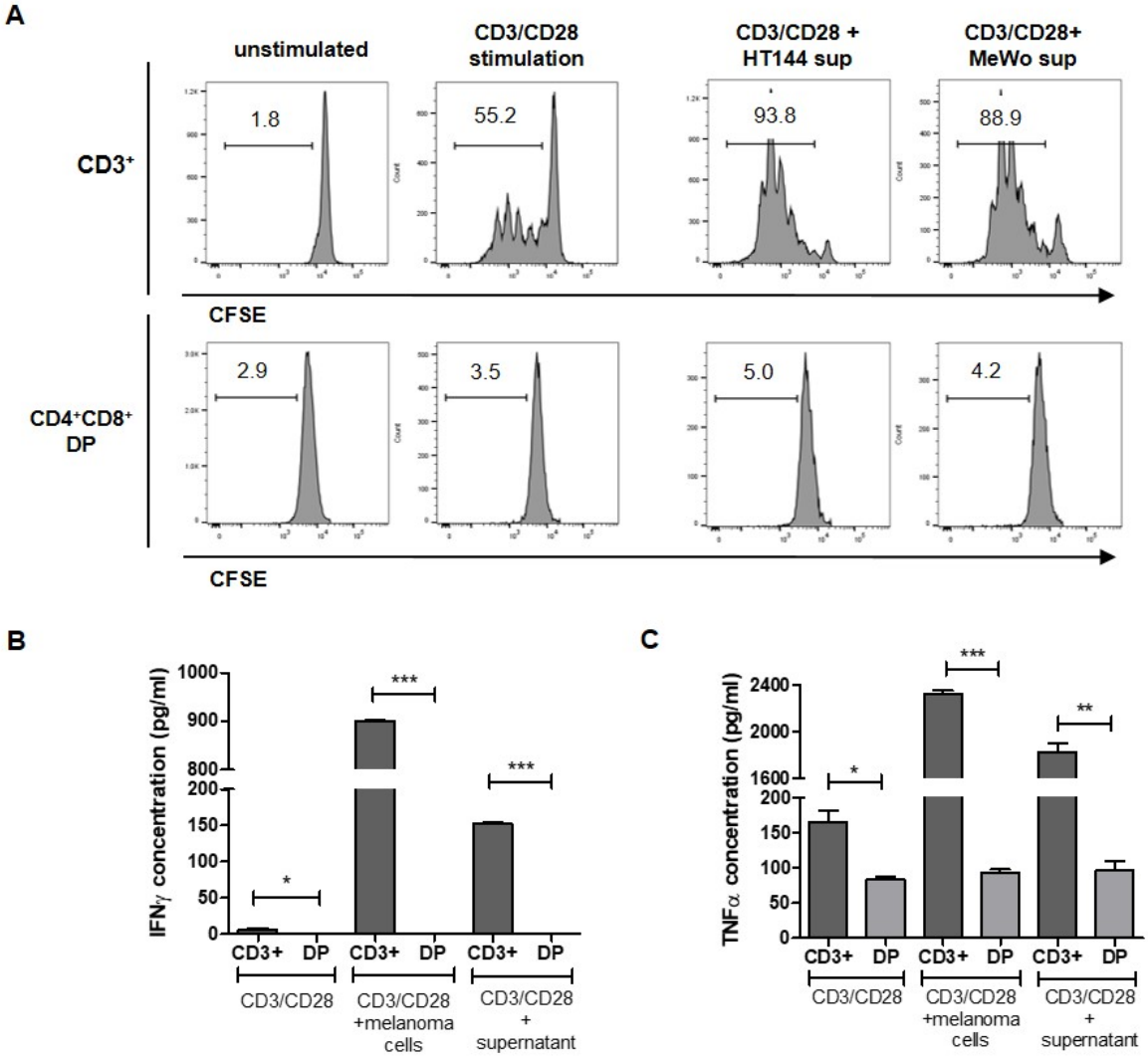

Fig. 14: Proliferation and cytokine secretion of differentiated $CD4^+CD8^+$ DP T cells compared to freshly isolated $CD3^+$ T cells from human PBMCs. **A** Histograms showing the percentage of proliferating CFSE-labeled freshly isolated $CD3^+$ T cells isolated from healthy donor PBMCs and differentiated $CD4^+CD8^+$ DP T cells (day40). Cells were stimulated with plate-bound anti-CD3/CD28 antibody and cultured with melanoma cell supernatant for 4 days before FACS analysis. As indicated supernatant from HT144 or MeWo melanoma cell lines was added, respectively. **B, C** Cytokine secretion from $CD3^+$ T cells isolated from healthy donor PBMCs and differentiated $CD4^+D8^+$ DP T cells (day40). Cells were stimulated with plate-bound anti-CD3/CD28 antibody and cultured with melanoma cells or supernatant from HT144 (IFNγ) or MeWo (TNFα) melanoma cell lines for 4 days. Supernatants were harvested and analyzed for IFNγ (B) and TNFα (C) concentration was quantified by ELISA. Data represent mean ± SEM *p < 0.05, **p < 0.01, ***p < 0.005.

4.11 Activation of $CD4^+CD8^+$ DP T cells with CD3/CD28/CD2 cocktail supplemented with IL-15 induced $CD8^+$ SP T cell differentiation

In the human thymus $CD4^+CD8^+$ DP T cells undergo positive and negative selection for maturation and becoming either $CD4^+$ or $CD8^+$ SP T cells. Here, the treatment with an activation cocktail containing CD3, CD28 and CD2 in combination with IL-15 for seven days was used to induce the differentiation of $CD8^+$ SP T cells from DP cells. As shown in Figure 15A, seven day treatment led to the development of $CD8^+$ SP MART-1- and MCSP-transfected cells as well as untransfected cells (HD11). For MART-1-transfected cells about 32.7 % of the total live population showed a $CD8^+CD4^-$ expression. Similar results were found for untransfected HD11 cells (34.3 %). For MCSP-transfected cells 14.3 % $CD8^+$ SP T cell were detected. On average, 32 % of the live untransfected HD11 cells were found to express $CD8^+$ ($CD4^-$) at day 47 of differentiation and about 20 % of the transfected cells (MART-1 and MCSP) with varying percentages between different experimental batches (Figure 15B). For the transfected cells (MART1 and MCSP) a higher amount of $CD4^+CD8^+$ DP T cells were found at day 47, which apparently did not differentiate further to the $CD8^+$ SP stage. The analysis of the expression of the T cell marker CD3 revealed that only 17.8 % of the $CD8^+$ SP MART-1-transfected cells and 0.8 % of the $CD8^+$ SP MCSP-transfected cells expressed CD3. In contrast, almost 100 % of the $CD8^+$ SP T cells were expressing leukocyte marker CD45. MCherry expression was detected in 28.2 % (MART1) or 89.5 % (MCSP) of the live population, respectively.

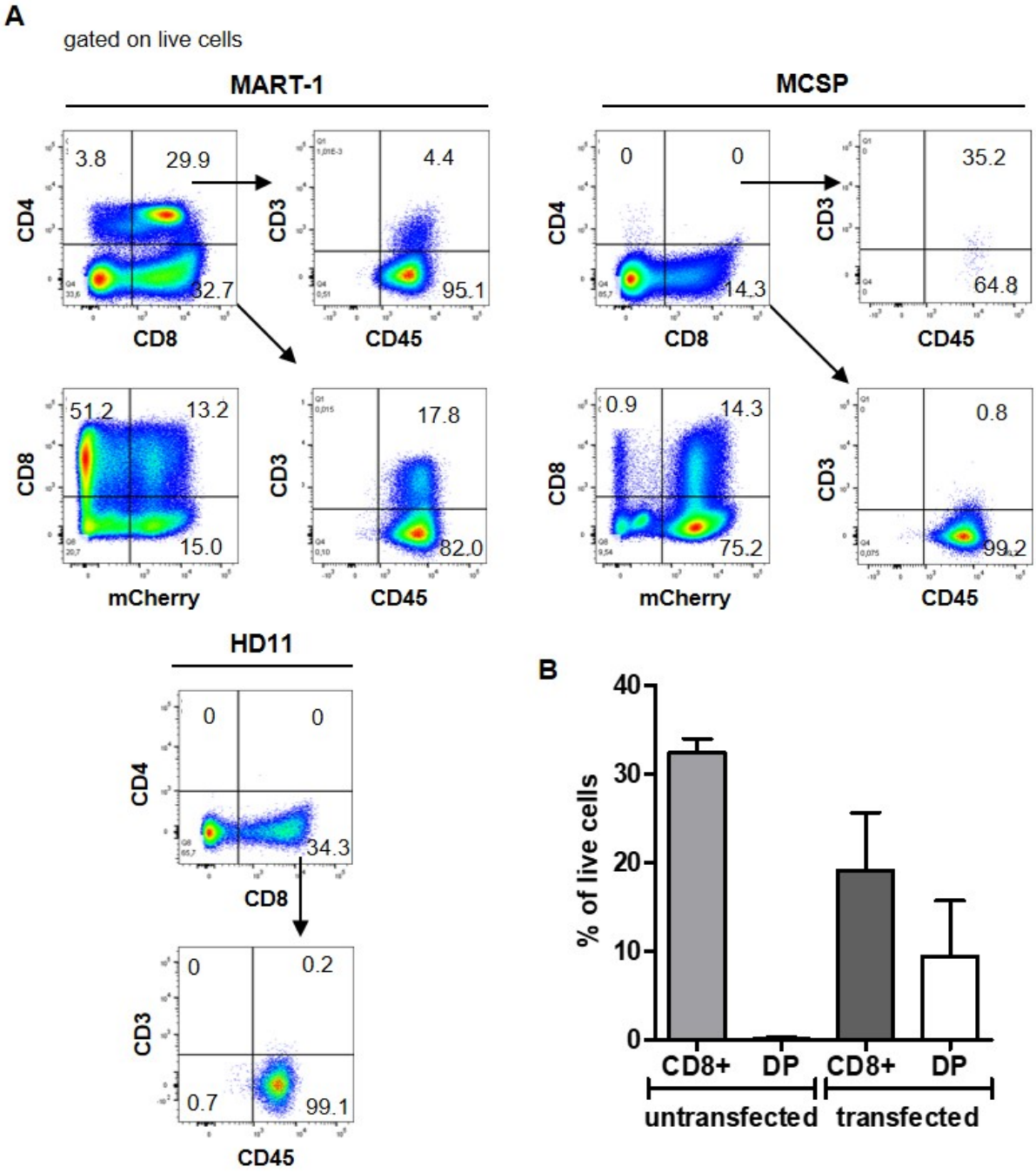

Fig. 15: Generation of CD8$^+$ SP T cells from CD4$^+$CD8$^+$ DP T cells. A Representative flow cytometry profile at day 47 of differentiation after gating on the total live cell population for MART-1- and MCSP-transfected cells as well as untransfected HD11 cells. Live cells were first analyzed for the expression of CD4, CD8 and further for T cell marker CD3 and leukocyte marker CD45. MCherry expression was quantified in the total live cell population and analyzed together with CD8 expression. **B** Diagram showing the percentage of CD8$^+$ SP and CD4$^+$CD8$^+$ DP T cells at day 47 of differentiation gated on live cells. Data represent mean ± SEM (n = 2-4). *$p < 0.05$.

4.12 Differentiated CD8$^+$ SP T cells showed IFNγ and CD107a expression after stimulation

Effector functions of CD8$^+$ T cells in anti-tumor immunity include the secretion of cytokines, granzymes and perforin. Also the upregulation of T cell activation markers like CD25 or CD69 and the production of IFNγ are effector T cell functions. To test the functionality of the generated CD8$^+$ SP T cells CD107a and intracellular IFNγ expression in response to stimulation with phorbol 12-myristate 13-acetate (PMA) and ionomycin (iono) for 4 hours were analyzed by FACS. As shown in Figure 16 the stimulation with PMA/iono induced IFNγ expression in CD3$^+$ T cells isolated from human PBMCs as well as in differentiated CD8$^+$ SP T cells. Similar results were found for the expression of CD107a as marker for degranulation. After PMA/iono stimulation the percentage of CD107a-expressing, differentiated CD8$^+$ SP T cells increased to 33.3 % compared to the unstimulated control (5.6 %). Taken together, compared to CD4$^+$CD8$^+$ DP T cells, differentiated CD8$^+$ SP T cells showed increased intracellular INFγ and CD107a levels after 47 days of differentiation and additional stimulation for 4 h with PMA/iono similar to CD3$^+$ cells.

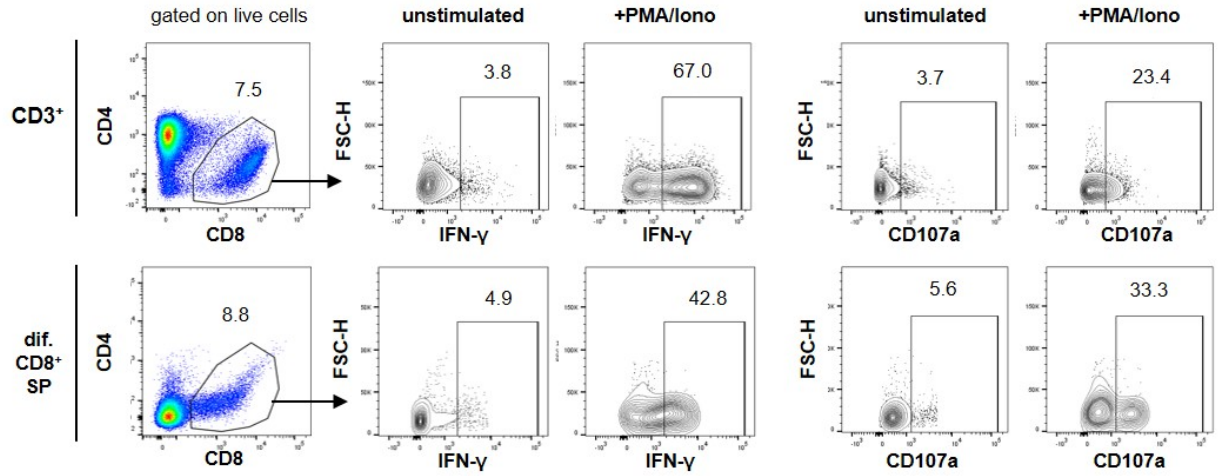

Fig. 16: IFNγ and CD107a expression of differentiated CD8$^+$ SP T cells after stimulation. Representative flow cytometry plots showing the intracellular expression of INFγ and surface CD107a from isolated CD3$^+$ (upper row) or differentiated CD8$^+$ SP T cells (lower row). Cells were either stimulated with PMA/iono for 4 h or unstimulated and treated with BFA after 1 h. CD4 and CD8 expression was investigated from total live population. Numbers indicate the percentage of positive cells.

4.13 Differentiated CD8$^+$ SP T cells showed anti-tumor effects against melanoma cell lines

To determine the anti-tumor effector function of the generated CD8$^+$ SP T cells melanoma cell lines C32 and WM266-4 expressing MART-1 and MCSP were used as target cells for cytotoxicity assays. MART-1- and MCSP-specific CD8$^+$ SP T cells were co-cultured in different ratios with melanoma cells, which were stained with CP-Dye450 (Biosciences) before. Cell viability of CP-Dye450-positive melanoma cells was assessed by PI staining after 24 or 48 h of co-culture, respectively. As shown in Figure 17A the percentage of PI-positive cells increased for both C32 and WM266-4 after the addition of MCSP-transfected CD8$^+$ SP T cells compared to only medium control. For C32 I did not observe a difference in the percentage of PI-positive cells between the 1:5 and 1:10 melanoma/T cell ratios. For WM266-4 a different result was observed. A higher ratio of T cells (1:10) caused a higher percentage of PI-positive cells compared to the lower ratio (1:5). However, already the lower ratio of MCSP-transfected CD8$^+$ T cells (1:5) induced a higher percentage of PI$^+$ WM266-4 cells compared to C32 cells. Therefore, generated MCSP-transfected CD8$^+$ T cells exerted a stronger cytotoxic effect against WM266-4 cell compared to C32 cells. An explanation for that could be found in the surface expression levels of MCSP on WM266-4 and C32 melanoma cells. FACS analysis revealed a higher surface expression of MCSP on WM266-4 cells compared to C32 cells (Supplementary Figure 18).

HLA typing of the cells revealed an HLA-A*02 allele for WM266-4 cells and HLA-A*01 allele for C32 (Supplementary Table 14). Since the MART-1 TCR is HLA-A*02 restricted, WM266-4 cells were chosen for the cytotoxicity assay with differentiated MART-1 CD8$^+$ SP T cells. As shown in Figure 17B, the percentage of PI-positive cells increased ratio dependent after co-cultering with MART-1-transfected CD8$^+$ SP T cells for 24 h compared to medium control or undifferentiated hiPSCs. The highest significant cytotoxic effect was found for a 1:20 melanoma/T cell ratio resulting in 36 % PI-positive WM266-4 cells. For a 1:5 or 1:10 melanoma/T cell ratio the effect was still not significant with about 15 % or 22 % PI-positive WM266-4 cells on average. In conclusion, differentiated CD8$^+$ SP T cells showed cytotoxic effects against melanoma cells after co-culture for 24 or 48 h. However, a high ratio of T to melanoma cells was necessary to see a significant effect.

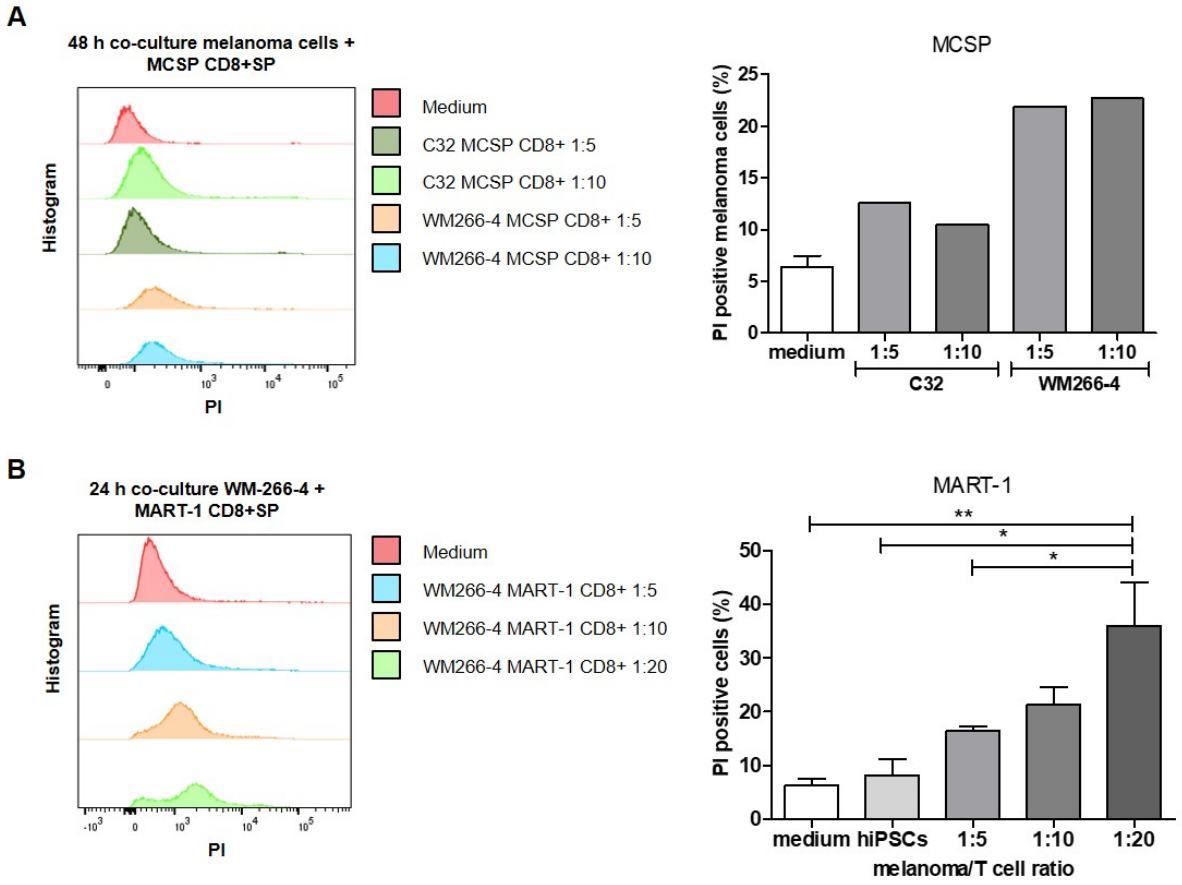

Fig. 17: Cytotoxicity assay with differentiated CD8$^+$ T cells and melanoma cells. A Histogram and bar diagram displaying the quantities of PI-positive melanoma cells (C32 or WM266-4) after co-culture with differentiated MCSP-transfected CD8$^+$ T cells. Cells were cultured in 24-well plates with different melanoma/ T cell ratios for 48 hours and stained with PI. Melanoma cells were stained with CP-Dye450 (Biosciences) beforehand for distinction. **B** Histogram and bar diagram displaying the distribution of PI-positive WM266-4 melanoma cells after co-culture with differentiated MART-1-transfected CD8$^+$ T cells. Cells were cultured in 24-well plates with different melanoma/ T cell ratios for 24 hours and stained with PI. Melanoma cells were stained with CP-Dye450 (Biosciences) beforehand for distinction. Data represent mean ± SEM (n = 2-4). *p < 0.05, **p < 0.01.

5 Discussion

Due to the high capacity to metastasize and to develop resistances against current therapies melanoma is one of the most aggressive skin cancer types. Together with the rising incidence of newly diagnosed melanoma cases every year the development of effective treatment strategies for patients is of very high demand [87]. Although adoptive cell therapies more and more replace common targeted or immune checkpoint therapies issues with sudden disease relapse still persist. Reasons for that are found in T cell dysfunction associated with exhaustion, senescence and decreased effector functions [88]. Moreover, the unlimited production of "off-the-shelf" T cells for allogeneic use is still difficult to achieve. By using hiPSCs as starting material, issues such as culture time restrictions or time dependent exhaustion could be overcome. Additionally it was shown, that iPSC-derived T cells have elongated telomers and a higher proliferative capacity [88, 89].

In this study, two possible methods for the generation of melanoma antigen-specific $CD8^+$ T cells from hiPSCs were examined. However, still existing difficulties and limits were revealed as well. A major point of this thesis was the use of S/MAR vectors to genetically modify hiPSCs so that they and their derivatives overexpress a melanoma antigen-specific TCR or CAR. I could show that $CD8^+$ SP T cells derived from those hiPSCs still expressed MART-1 TCR or MCSP CAR, respectively, after 47 days of differentiation. This fact suggests that no epigenetic DNA vector silencing occured during the process of differentiation. Using common feeder-based co-culture systems the generation of $CD4^+CD8^+$ DP T cells was successful. However further differentiation towards the $CD8^+$ SP stage remained difficult. On the other hand, the use of a commercially available kit from Stemcell Technologies enabled the generation of $CD8^+$ SP T cells showing effector functions. Nevertheless, the amount of generated $CD8^+$ SP T cells was still quite low and therefore not ideal for further clinical applications, especially because of the fact that common adoptive T cell transfers require up to 10^{10} T cells for one single infusion at the moment [90]. Further limitations as well as accomplishments and alternatives for improvement were discussed in the following sections.

5.1 S/MAR DNA vectors as gene delivery systems

S/MAR DNA vectors are known for their resilience to epigenetic silencing during differentiation processes and for their property to be stably passed on from mother to daughter cell over many cell divisions although not being incorporated into the genome of the host cell. For that reason, they represent promising and safe alternatives to viral vectors for future gene therapies. S/MAR

DNA vectors coding for the MART-1 TCR or a MCSP CAR, respectively, and the reporter gene were used in this study. Since S/MAR vectors do not integrate into the host genome like viral vectors such as lentiviruses they do not randomly modify the host genome. Instead, the unique S/MAR element promotes the specific binding of the vector to the chromosomal scaffold during the mitotic phase and enables consistent transgene expression [91]. However, further antibiotic or reporter gene selection is required to generate cell lines stably expressing the GOI. Here, I found that during the first FACS-based cell sort 6 dpt between 8 % and 33 %cof live cells expressed the GOI. After that first sort the percentage of mCherry-positive cells dropped immensely to less than 1 % as revealed during the second sort 19 days after transfection. This could be explained by the fact that S/MAR DNA vectors need to find the right nuclear location close to a transcription factory, which provides an active transcription of the GOI encoded by the vector [92, 93]. The high loss of expression might be due to an unfavorable location of the vector distant to a transcription factory. However, as soon as the vector was located at an advantageous location, here after the third FACS-based cell sort, a stable expression was achieved that still persisted after repeated cycles of freezing and thawing of the hiPSCs. Therefore, I conclude that S/MAR DNA vectors are a suitable tool for genetic modification of hiPSCs taking into account that several rounds of cell sorting were necessary to generate a stable expression of the GOI.

Upon transfection, gene expression levels of common pluripotency markers NANOG, OCT4 and SOX2 were quantified in order to rule out that the transfection process interferes with endogenous gene expression. As expected, transfection with the S/MAR DNA vectors did not have an overall suppressing or stimulating effect on the expression levels of all the pluripotency genes. Only the expression of SOX2 was significantly decreased in MART-1-transfected as well as in MCSP-transfected cells. However, since the three factors control gene expression in a co-operative way to maintain pluripotency the decreased SOX2 expression might be a result of the relatively low sample size (n = 3). Especially, since SOX2 forms a binary complex together with OCT4, whose expression level was not decreased [94, 95].

After subjecting the transfected hiPSCs to differentiation towards the HSPC lineage, I also examined if the gene expression levels of T cell-related differentiation genes could be affected by the transfection with the S/MAR constructs. Therefore, gene expression levels of representative genes in isolated $CD34^+$ HSPCs after 9 days of co-culture on OP9 cells were determined. The highest difference in the expression levels between transfected and untransfected cells was found for LEF1 and NOTCH1. LEF1 promotes the β-selection at the DN3/4 stage together with TCF1 [86]. However, both TFs also play a role in the establishment of $CD8^+$ T cell identity through suppression of $CD4^+$ T cell development [96]. As described by Dik *et al.* the highest LEF1 gene expression is not

found at the the $CD34^+$ HSPC stage of T cell development but at the $CD8^+$ SP stage at day 42 [97]. Taking the low expression levels of LEF1 into account, little changes could lead to significant differences between the untransfected and transfected cells. This hypothesis is also supported by the fact that the expression levels of TCF7, which encodes the TF TCF1 that interacts together LEF1, did not show strong differences between both groups. Differences between MART-1-transfected and untransfected cells were also found for the expression of NOTCH1. However, as indicated by the long error bar, the expression levels differed a lot between experimental replicates and further repetitions would be necessary to make a clear statement. After all, I conclude that there was no significant difference in the expression levels of T cell related genes between transfected and untransfected cells at the $CD34^+$ HSPC stage and that observed variations might be a result of a relatively small sample size. For further conclusions, I would suggest to increase the sample size but also to include later developmental stages lik $CD4^+CD8^+$ DP T cells into the analysis. Furthermore, the expressions of additional genes such as BCL11b, which is a key regulator of thymocyte differentiation and survival might be revealing [98].

5.2 OP9 stromal cells for the induction of the hematopoietic specification

The first approach used in this study to generate T cells from hiPSCs was focused on the hematopoietic specification. In detail, OP9 stromal cells originally derived from murine bone marrow were used for the differentiation of $CD34^+$ HSPCs from hiPSCs. After 9 days of co-culture, $CD34^+$ HSPCs could be isolated from the cell suspension by FACS or immunomagnetic separation. Both methods worked equally well, but the purity of the isolated cell populations was usually higher using FACS. However, a higher viability of the cells as well as a decreased influence on cell activity was reported for magnetic separation compared to FACS [99]. In general, previous studies have shown that magnetic separation is a suitable method for T cell isolation and much more flexible and less time consuming than FACS [100]. For that reason, magnetic separation was performed in this study since it is also the method of choice in the protocol of the T cell differentiation kit (Stemcell Technologies).

5.3 OP9 stromal cells and alternative methods for the generation of T cells from HSPCs

For subsequent medical applications of in vitro generated T cells, contamination with other cell types would be a big impediment. However, the co-culture methods rely on OP9 feeder cells and even using FACS to enrich the T cell population does not guarantee that it is free of OP9 feeder cells. For that reason a differentiation method using murine stromal cells is not suitable for further clinical applications of the differentiated T cells. Nevertheless, the majority of publications report the use of stromal cells expressing the NOTCH ligands DLL1 or DLL4 for the generation of T cells from HSPCs in combination with additional factors as IL-7, FLT3L, SCF and chemokines like CXCL12 and CCL25 [101]. By using OP9-FS12 cells I was able to generate $CD4^+CD8^+$ DP T cells from $CD34^+$ HSPCs. However, I did not success in generating CD8+ SP T cells. Reasons for that might be the missing activation step that was applied to the $CD4^+CD8^+$ DP T cells generated with the T cell differentiation kit from StemCell Technologies using CD3/CD28/CD2. In human thymus the development of $CD8^+$ SP T cells from $CD4^+CD8^+$ DP T cells is accomplished by positive/negative selection in specified selection niches containing different types of antigen presenting cells (APCs) like TECs and DCs [102]. The *in vitro* recreation of those niches comprising APCs in a three dimensional context is not feasible at the moment and makes the selection part more difficult. Organoid-based T cell differentiation methods recently published by Seet et al. and Montel-Hagen et el. provide great opportunities to study T cell development *in vitro* [63, 103, 104]. However, even T cells generated with this approach lack *in vivo* immunocompetence after engraftment [104]. For that reason, Guo *et al.* focused on the coordinated expression of defined TFs to enable T lymphopoiesis *in vivo* [104]. However, this study was performed with murine cells.

On the other hand, recent studies focus on the substitution of OP9 cells since clinical applications with feeder-based differentiation systems stay challenging. Iriguchi *et al.* demonstrated a feeder-free differentiation culture system based on the formation of EBs followed by a 3 week long culture on immobilized-DLL4 protein coated plates and a 7 day long activation with CD3 antibody [105]. With this method a big step in the production of "off-the-shelf" T cells for allogeneic T cell therapy was made. However, a major complication of the allogeneic application of hiPSC-derived $CD8^+$ T cells are possible HLA mismatches which could lead to immune rejections or GvHD [105].

5.4 HLA as limiting factor for "off-the-shelf" immunotherapy?

HLA class I molecules comprise HLA-A, -B, -C and are expressed on all nucleated cells. HLA class I molecules are recognized by $CD8^+$ T cells and facilitate the presentation of endogenously processed antigens [106]. HLA phenotyping of the cells used in this study revealed the HLA-A*11:01 allele for the hiPSCs, HLA-A*01:01 for C32 melanoma cells and HLA-A*02:01 for WM266-4 melanoma cells (see supplementary Table 13). The MART-1 TCR received from Michael Nishimura is HLA-A*02 restricted and recognizes the immuno-dominant 27-35 epitope AAGIGILTV. For that reason only HLA-A*02:01 WM266-4 cells were used for the cytotoxicity assay with the generated MART-1-transfected $CD8^+$ SP T cells to ensure HLA-A matching. I could show that the MART-1-transfected $CD8^+$ SP T cells induced a significant increase of the percentage of PI^+ WM266-4 cells after 24 h. In order to see an even higher cytotoxic effect I suggest to increase the melanoma/T cell ratio up to 1:40. Especially because of the fact that the cells harvested at day 47 of differentiation were not sorted for the presence of CD8. Cell sorting would improve the purity of the cell population by removing undifferentiated and dead cells. For MCSP-transfected $CD8^+$ SP T cells the yield at day 47 was not as high and only lower melanoma/T cell ratios could be used for the cytotoxicity assay. Compared to the 1:20 ratio used for MART-1-transfected T cells the 1:5 as well as the 1:10 ratio did not have a significant effect on the viability of the melanoma cells. Nevertheless, I observed a trend that the percentage of PI-positive cells was higher for WM266-4 compared to C32 cells. A reason for that could be the higher surface expression of MCSP on WM266-4 compared to C32 cells as demonstrated by FACS analysis (supplementary Figure 18). Therefore, I would suggest that additional cytotoxicity experiments should only include WM266-4 since the cell yield is still limited. However, the melanoma/T cell ratio should be increased to at least 1:20, if possible.

For future clinical applications the HLA-A allele of the original hiPSCs should match with the HLA-A allele of the treated patient regardless of whether TCR- or CAR-transfected cells are used. Of course, one idea would be to create hiPSC stocks isolated from HLA homozygous donors, which cover the most common HLA-A types. However, this would require an enormous screening effort. Another solution reported by Xu *et al.* suggests the use of genome-editing technologies to generate immuno-compatible donor hiPSCs by disruption of both HLA-A and -B alleles to maintain antigen presentation but suppress the response of NK cells [106]. Moreover, previous publications already described the knock out of the β2-microglobulin (B2M) gene, which is required for HLA class I presentation on the cell surface and thereby preventing $CD8^+$ T cell-induced immune responses [107–109]. In conclusion, the integration of the aforementioned HLA editing techniques would be required to enable the allogeneic use of hiPSC-derived $CD8^+$ T cells in clinical applications. Even

so recent studies investigated possible ways to circumvent HLA mismatches there is still room for improvement.

5.5 CD3 expression on differentiated $CD4^+CD8^+$ DP and CD8 SP T cells

T cell marker expression including CD3, CD4 and CD8 was analyzed by FACS at day 40 and day 47 of differentiation. Unexpectedly, less than 20 % of the $CD4^+CD8^+$ DP T cells at day 40 and $CD8^+$ SP T cells at day 47 were expressing CD3. For differentiated MCSP-transfected $CD8^+$ SP T cells the percentage of $CD3^+$ cells was just around 1 %. CD3 is part of the T cell antigen receptor complex, consisting of the TCR α and β chain for the recognition of the peptide–MHC complex and the CD3 signaling complex, which is made up of the CD3$\gamma\epsilon$, CD3$\delta\epsilon$ and CD$\zeta\zeta$ dimers [110, 111]. It is known that the rearrangement of the TCRβ genes of the later TCR/CD3 complex already takes place at the DN stage of T cell development followed by the expression of a pre-TCR on the cell surface. Signaling through this pre-TCR/CD3 complex induces the maturation of $CD4^+CD8^+$ DP T cells. Those DP T cells undergo another selection of the TCR/CD3 complex where TCRα genes are rearranged leading to maturation of $CD4^+$ or $CD8^+$ SP thymocytes. For that reason, both $CD4^+CD8^+$ DP and $CD8^+$ SP T cells were supposed to express CD3. [112]. Since that was not the case here, I hypothesize that the rearrangement of the TCRβ genes at the DN stage of T cell development went wrong. Van der Stegen *et al.* reported similar observations recently for the generation of T cells from iPSCs [113]. In detail, it was shown, that the premature CAR expression at the early DN stage of T cell development obstructed the Notch signaling and promoted the differentiation of an innate-like phenotype. Therefore, DLL4 was not longer able to induce the transition from the DN to the DP stage of $\alpha\beta$T cells and instead promoting an innate-like CD8$\alpha\alpha$ or NK-like phenotype [114, 115].

It would be interesting to investigate the impact of the TCR/CAR on the expression of endogenous TCRs using TCR sequencing at different stages of differentiation, e.g. at the $CD4^+CD8^+$ DP stage as well as at the $CD8^+$ SP stage.

Although lacking CD3 expression, I found that the generated $CD8^+$ SP T cells were able to secrete IFNγ and to upregulate CD107a after PMA/iono stimulation. In general, the activation of T cells via PMA/iono does not work via the TCR/CD3 complex. Instead, the activation of protein kinase C by PMA and the function of ionomycin as calcium ionophore induce the stimulation of several intracellular signaling pathways for cytokine production [116]. To see a specific TCR-dependent activation the use of MART-1 tetramers would be useful. For the activation of the MCSP CAR

T cells the recombinant antigen could be either plate-bound or nanobead-bound to induce an activation. For both receptors the application of engineered target cell lines expressing the specific antigen could be another idea [117]. However, already the ability of the generated T cells to express IFNγ and CD107a after nonspecific stimulation proves the functionality to a certain extent.

6 Conclusion and Outlook

In summary, the *in vitro* generation of hiPSC derived cancer antigen-specific $CD8^+$ SP T cells for immunotherapeutic applications is a promising approach for the treatment of cancer patients. Here, I investigated two different strategies for the differentiation of hiPSCs expressing MART-1 TCR or MCSP CAR, respectively, into $CD8^+$ SP T cells via the hematopoietic stage. The first approach comprised the long-term co-culture with bioengineered OP9 stromal cells from $CD34^+$ HSPCs. I was able to generate $CD4^+CD8^+$ DP T cells after 35 days of co-culture but did not succeed in the generation of $CD8^+$ SP T cells. The replacement of the OP9 cells by a T cell differentiation kit (Stemdiff, Stemcell Technologies) enabled the generation of $CD8^+$ SP T cells after 47 days. Even though the generated $CD8^+$ SP T cells did not show a high expression of T cell marker CD3, I was able to detect intracellular expression of IFNγ and surface expression of CD107a after stimulation. On the other hand, cytotoxic effects of the generated $CD8^+$ SP T cells were observed after co-culture with melanoma cell lines.

All in all, I could successfully generate $CD8^+$ SP T cells expressing MART-1 TCR or MCSP CAR via $CD34^+$ HSPCs from hiPSCs. However, one major point for improvement is to increase the cell yield at day 47 of differentiation. Therefore, common differentiation methods need to be revised and possible alternatives reviewed. Additionally, it is needed to examine why there was only low expression of CD3, which was already observed at the $CD4^+CD8^+$ DP stage of T cell development (day 40). For future potential clinical applications questions regarding the HLA match between the donor cells and the recipient must be solved.

It only remains to add, that the generation of $CD8^+$ T cells from hiPSCs in combination with the use of S/MAR DNA vectors is a promising approach for the improvement of adoptive cell therapy. However, several hurdles must still be overcome until patients can be finally treated with those cells.

Bibliography

1. Domingues, B., Lopes, J. M., Soares, P. & Pópulo, H. Melanoma treatment in review. *Immunotargets Ther* **7,** 35–49 (2018).
2. World Health Organization. *Melanoma of Skin.* https://gco.iarc.fr/today/data/factsheets/cancers/16-Melanoma-of-skin-fact-sheet.pdf. Accessed: 06.07.2022. (2020).
3. American Cancer Society. *Cancer Facts & Figures 2018.* https://www.cancer.org/content/dam/cancer-org/research/cancer-facts-and-statistics/annual-cancer-facts-and-figures/2018/cancer-facts-and-figures-2018.pdf. Accessed: 06.07.2022. (2018).
4. World Cancer Research Funds International. *Skin cancer statistics.* https://www.wcrf.org/cancer-trends/skin-cancer-statistics/. Accessed: 06.07.2022. (2022).
5. American Cancer Society. *Key Statistics for Melanoma Skin Cancer.* https://www.cancer.org/cancer/melanoma-skin-cancer/about/key-statistics.html. Accessed: 14.07.2022. 2022.
6. Karimi, K., Lindgren, T. H., Koch, C. A. & Brodell, R. T. Obesity as a risk factor for malignant melanoma and non-melanoma skin cancer. *Reviews in Endocrine and Metabolic Disorders* **17,** 389–403 (2016).
7. American Cancer Society. *Risk Factors for Melanoma Skin Cancer.* https://www.cancer.org/cancer/melanoma-skin-cancer/causes-risks-prevention/risk-factors.html. Accessed: 06.07.2022. (2021).
8. American Cancer Society. *Survival Rates for Melanoma Skin Cancer.* https://www.cancer.org/cancer/melanoma-skin-cancer/detection-diagnosis-staging/survival-rates-for-melanoma-skin-cancer-by-stage.html. Accessed: 14.07.2022. (2022).
9. Sandru, A., Voinea, S., Panaitescu, E. & Blidaru, A. Survival rates of patients with metastatic malignant melanoma. *J Med Life* **7,** 572–6 (2014).
10. Shain, A. H. & Bastian, B. C. From melanocytes to melanomas. *Nature Reviews Cancer* **16,** 345–358 (2016).
11. Wellbrock, C. in *From Melanocytes to Melanoma: The Progression to Malignancy* (eds Hearing, V. J. & Leong, S. P. L.) 247–263 (Humana Press, Totowa, NJ, 2006).

12. Eddy, K., Shah, R. & Chen, S. Decoding Melanoma Development and Progression: Identification of Therapeutic Vulnerabilities. *Frontiers in Oncology* **10** (2021).

13. Paluncic, J. *et al.* Roads to melanoma: Key pathways and emerging players in melanoma progression and oncogenic signaling. *Biochimica et Biophysica Acta (BBA) - Molecular Cell Research* **1863,** 770–784 (2016).

14. Davis, E. J., Johnson, D. B., Sosman, J. A. & Chandra, S. Melanoma: What do all the mutations mean? *Cancer* **124,** 3490–3499 (2018).

15. Curti, B. D. & Faries, M. B. Recent Advances in the Treatment of Melanoma. *New England Journal of Medicine* **384,** 2229–2240 (2021).

16. Jiang, G., Li, R. H., Sun, C., Liu, Y. Q. & Zheng, J. N. Dacarbazine combined targeted therapy versus dacarbazine alone in patients with malignant melanoma: a meta-analysis. *PLoS One* **9,** e111920 (2014).

17. Kim, C., Lee, C. W., Kovacic, L., Shah, A., Klasa, R. & Savage, K. J. Long-term survival in patients with metastatic melanoma treated with DTIC or temozolomide. *Oncologist* **15,** 765–71 (2010).

18. Wilson, M. A. & Schuchter, L. M. in *Melanoma* (eds Kaufman, H. L. & Mehnert, J. M.) 209–229 (Springer International Publishing, Cham, 2016).

19. Tanda, E. T., Vanni, I., Boutros, A., Andreotti, V., Bruno, W., Ghiorzo, P. & Spagnolo, F. Current State of Target Treatment in BRAF Mutated Melanoma. *Frontiers in Molecular Biosciences* **7** (2020).

20. Chapman, P. B. *et al.* Improved survival with vemurafenib in melanoma with BRAF V600E mutation. *N Engl J Med* **364,** 2507–16 (2011).

21. Wong, D. J. L. & Ribas, A. in *Melanoma* (eds Kaufman, H. L. & Mehnert, J. M.) 251–262 (Springer International Publishing, Cham, 2016).

22. Subbiah, V., Baik, C. & Kirkwood, J. M. Clinical Development of BRAF plus MEK Inhibitor Combinations. *Trends in Cancer* **6,** 797–810 (2020).

23. Zhang, Y. & Zhang, Z. The history and advances in cancer immunotherapy: understanding the characteristics of tumor-infiltrating immune cells and their therapeutic implications. *Cellular Molecular Immunology* **17,** 807–821 (2020).

24. Andtbacka, R. H. *et al.* Talimogene Laherparepvec Improves Durable Response Rate in Patients With Advanced Melanoma. *Journal of Clinical Oncology* **33,** 2780–2788 (2015).

25. Pol, J., Kroemer, G. & Galluzzi, L. First oncolytic virus approved for melanoma immunotherapy. *OncoImmunology* **5,** e1115641 (2016).

26. Zitvogel, L., Galluzzi, L., Kepp, O., Smyth, M. J. & Kroemer, G. Type I interferons in anticancer immunity. *Nature Reviews Immunology* **15,** 405–414 (2015).

27. Jiang, T., Zhou, C. & Ren, S. Role of IL-2 in cancer immunotherapy. *Oncoimmunology* **5,** e1163462 (2016).

28. Leach, D. R., Krummel, M. F. & Allison, J. P. Enhancement of antitumor immunity by CTLA-4 blockade. *Science* **271,** 1734–6 (1996).

29. Leonardi, G. C., Candido, S., Falzone, L., Spandidos, D. A. & Libra, M. Cutaneous melanoma and the immunotherapy revolution (Review). *Int J Oncol* **57,** 609–618 (2020).

30. Hodi, F. S. *et al.* Improved survival with ipilimumab in patients with metastatic melanoma. *N Engl J Med* **363,** 711–23 (2010).

31. Huang, A. C. & Zappasodi, R. A decade of checkpoint blockade immunotherapy in melanoma: understanding the molecular basis for immune sensitivity and resistance. *Nature Immunology* **23,** 660–670 (2022).

32. Carlino, M. S., Larkin, J. & Long, G. V. Immune checkpoint inhibitors in melanoma. *Lancet* **398,** 1002–1014 (2021).

33. Wolchok, J. D. *et al.* Long-Term Outcomes With Nivolumab Plus Ipilimumab or Nivolumab Alone Versus Ipilimumab in Patients With Advanced Melanoma. *J Clin Oncol* **40,** 127–137 (2022).

34. Rohatgi, A. & Kirkwood, J. M. Beyond PD-1: The Next Frontier for Immunotherapy in Melanoma. *Frontiers in Oncology* **11** (2021).

35. Tawbi, H. A. *et al.* Relatlimab and Nivolumab versus Nivolumab in Untreated Advanced Melanoma. *New England Journal of Medicine* **386,** 24–34 (2022).

36. Rosenberg, S. A. & Restifo, N. P. Adoptive cell transfer as personalized immunotherapy for human cancer. *Science* **348,** 62–68 (2015).

37. Rosenberg, S. A. *et al.* Use of Tumor-Infiltrating Lymphocytes and Interleukin-2 in the Immunotherapy of Patients with Metastatic Melanoma. *New England Journal of Medicine* **319,** 1676–1680 (1988).

38. Restifo, N. P., Dudley, M. E. & Rosenberg, S. A. Adoptive immunotherapy for cancer: harnessing the T cell response. *Nature Reviews Immunology* **12,** 269–281 (2012).

39. Leko, V. & Rosenberg, S. A. Identifying and Targeting Human Tumor Antigens for T Cell-Based Immunotherapy of Solid Tumors. *Cancer Cell* **38,** 454–472 (2020).

40. Price, M. A. *et al.* CSPG4, a potential therapeutic target, facilitates malignant progression of melanoma. *Pigment Cell Melanoma Res* **24,** 1148–57 (2011).

41. Van Ewijk, W. *et al.* Thymic microenvironments, 3-D versus 2-D? *Semin Immunol* **11,** 57–64 (1999).

42. Haynes, B. F. & Heinly, C. S. Early human T cell development: analysis of the human thymus at the time of initial entry of hematopoietic stem cells into the fetal thymic microenvironment. *J Exp Med* **181,** 1445–58 (1995).

43. Park, J. E. *et al.* A cell atlas of human thymic development defines T cell repertoire formation. *Science* **367** (2020).

44. Rossi, F. M., Corbel, S. Y., Merzaban, J. S., Carlow, D. A., Gossens, K., Duenas, J., So, L., Yi, L. & Ziltener, H. J. Recruitment of adult thymic progenitors is regulated by P-selectin and its ligand PSGL-1. *Nat Immunol* **6,** 626–34 (2005).

45. Calderón, L. & Boehm, T. Three chemokine receptors cooperatively regulate homing of hematopoietic progenitors to the embryonic mouse thymus. *Proc Natl Acad Sci U S A* **108,** 7517–22 (2011).

46. Pievani, A. *et al.* Harnessing Mesenchymal Stromal Cells for the Engineering of Human Hematopoietic Niches. *Front Immunol* **12,** 631279 (2021).

47. Alves, N. L. *et al.* Characterization of the thymic IL-7 niche in vivo. *Proc Natl Acad Sci U S A* **106,** 1512–7 (2009).

48. Ciofani, M. & Zúñiga-Pflücker, J. C. A survival guide to early T cell development. *Immunol Res* **34,** 117–32 (2006).

49. Yu, Q., Sharma, A. & Sen, J. M. TCF1 and β-catenin regulate T cell development and function. *Immunologic Research* **47,** 45–55 (2010).

50. Famili, F., Wiekmeijer, A.-S. & Staal, F. J. The development of T cells from stem cells in mice and humans. *Future Science OA* **3,** FSO186 (2017).

51. Koch, U. *et al.* Delta-like 4 is the essential, nonredundant ligand for Notch1 during thymic T cell lineage commitment. *J Exp Med* **205,** 2515–23 (2008).

52. Thompson, P. K. & Zúñiga-Pflücker, J. C. On becoming a T cell, a convergence of factors kick it up a Notch along the way. *Semin Immunol* **23,** 350–9 (2011).

53. Anderson, G. & Takahama, Y. Thymic epithelial cells: working class heroes for T cell development and repertoire selection. *Trends Immunol* **33,** 256–63 (2012).

54. Röpke, C. Thymic epithelial cell culture. *Microsc Res Tech* **38,** 276–86 (1997).

55. Masuda, K., Germeraad, W. T., Satoh, R., Itoi, M., Ikawa, T., Minato, N., Katsura, Y., van Ewijk, W. & Kawamoto, H. Notch activation in thymic epithelial cells induces development of thymic microenvironments. *Mol Immunol* **46,** 1756–67 (2009).

56. Corbeaux, T., Hess, I., Swann, J. B., Kanzler, B., Haas-Assenbaum, A. & Boehm, T. Thymopoiesis in mice depends on a Foxn1-positive thymic epithelial cell lineage. *Proc Natl Acad Sci U S A* **107,** 16613–8 (2010).

57. Schmitt, T. M. & Zúñiga-Pflücker, J. C. Induction of T Cell Development from Hematopoietic Progenitor Cells by Delta-like-1 In Vitro. *Immunity* **17,** 749–756 (2002).

58. Kodama, H., Nose, M., Niida, S., Nishikawa, S. & Nishikawa, S. Involvement of the c-kit receptor in the adhesion of hematopoietic stem cells to stromal cells. *Exp Hematol* **22,** 979–84 (1994).

59. La Motte-Mohs, R. N., Herer, E. & Zuniga-Pflucker, J. C. Induction of T-cell development from human cord blood hematopoietic stem cells by Delta-like 1 in vitro. *Blood* **105,** 1431–9 (2005).

60. Schmitt, T. M., de Pooter, R. F., Gronski, M. A., Cho, S. K., Ohashi, P. S. & Zuniga-Pflucker, J. C. Induction of T cell development and establishment of T cell competence from embryonic stem cells differentiated in vitro. *Nat Immunol* **5,** 410–7 (2004).

61. Patel, E., Wang, B., Lien, L., Wang, Y., Yang, L. J., Moreb, J. S. & Chang, L. J. Diverse T-cell differentiation potentials of human fetal thymus, fetal liver, cord blood and adult bone marrow CD34 cells on lentiviral Delta-like-1-modified mouse stromal cells. *Immunology* **128,** e497–505 (2009).

62. Mohtashami, M. & Zúñiga-Pflücker, J. C. Three-dimensional architecture of the thymus is required to maintain delta-like expression necessary for inducing T cell development. *J Immunol* **176,** 730–4 (2006).

63. Seet, C. S. *et al.* Generation of mature T cells from human hematopoietic stem and progenitor cells in artificial thymic organoids. *Nat Methods* **14,** 521–530 (2017).

64. Takahashi, K. & Yamanaka, S. Induction of pluripotent stem cells from mouse embryonic and adult fibroblast cultures by defined factors. *Cell* **126,** 663–76 (2006).

65. Shi, Y., Inoue, H., Wu, J. C. & Yamanaka, S. Induced pluripotent stem cell technology: a decade of progress. *Nature Reviews Drug Discovery* **16,** 115–130 (2017).

66. Induced Pluripotent Stem Cells: Reprogramming Platforms and Applications in Cell Replacement Therapy. *BioResearch Open Access* **9,** 121–136 (2020).

67. Maherali, N. & Hochedlinger, K. Guidelines and Techniques for the Generation of Induced Pluripotent Stem Cells. *Cell Stem Cell* **3,** 595–605 (2008).

68. Stadtfeld, M., Nagaya, M., Utikal, J., Weir, G. & Hochedlinger, K. Induced Pluripotent Stem Cells Generated Without Viral Integration. *Science* **322,** 945–949 (2008).

69. Malik, N. & Rao, M. S. in *Pluripotent Stem Cells: Methods and Protocols* (eds Lakshmipathy, U. & Vemuri, M. C.) 23–33 (Humana Press, Totowa, NJ, 2013).

70. Robinton, D. A. & Daley, G. Q. The promise of induced pluripotent stem cells in research and therapy. *Nature* **481,** 295–305 (2012).

71. Brouwer, M., Zhou, H. & Nadif Kasri, N. Choices for Induction of Pluripotency: Recent Developments in Human Induced Pluripotent Stem Cell Reprogramming Strategies. *Stem Cell Reviews and Reports* **12,** 54–72 (2016).

72. Singh, V. K., Kalsan, M., Kumar, N., Saini, A. & Chandra, R. Induced pluripotent stem cells: applications in regenerative medicine, disease modeling, and drug discovery. *Frontiers in Cell and Developmental Biology* **3** (2015).

73. Kim, J. Y., Nam, Y., Rim, Y. A. & Ju, J. H. Review of the Current Trends in Clinical Trials Involving Induced Pluripotent Stem Cells. *Stem Cell Reviews and Reports* **18,** 142–154 (2022).

74. Deinsberger, J., Reisinger, D. & Weber, B. Global trends in clinical trials involving pluripotent stem cells: a systematic multi-database analysis. *npj Regenerative Medicine* **5,** 15 (2020).

75. Assawachananont, J., Mandai, M., Okamoto, S., Yamada, C., Eiraku, M., Yonemura, S., Sasai, Y. & Takahashi, M. Transplantation of Embryonic and Induced Pluripotent Stem Cell-Derived 3D Retinal Sheets into Retinal Degenerative Mice. *Stem Cell Reports* **2,** 662–674 (2014).

76. Sharma, A., Sances, S., Workman, M. J. & Svendsen, C. N. Multi-lineage Human iPSC-Derived Platforms for Disease Modeling and Drug Discovery. *Cell Stem Cell* **26,** 309–329 (2020).

77. Argyros, O., Wong, S. P. & Harbottle, R. P. Non-viral episomal modification of cells using S/MAR elements. *Expert Opin Biol Ther* **11,** 1177–91 (2011).

78. Stehle, I. M., Postberg, J., Rupprecht, S., Cremer, T., Jackson, D. A. & Lipps, H. J. Establishment and mitotic stability of an extra-chromosomal mammalian replicon. *BMC Cell Biol* **8,** 33 (2007).

79. Mirkovitch, J., Mirault, M. E. & Laemmli, U. K. Organization of the higher-order chromatin loop: specific DNA attachment sites on nuclear scaffold. *Cell* **39,** 223–32 (1984).

80. Bozza, M. *et al.* A nonviral, nonintegrating DNA nanovector platform for the safe, rapid, and persistent manufacture of recombinant T cells. *Sci Adv* **7** (2021).

81. Piechaczek, C., Fetzer, C., Baiker, A., Bode, J. & Lipps, H. J. A vector based on the SV40 origin of replication and chromosomal S/MARs replicates episomally in CHO cells. *Nucleic Acids Res* **27,** 426–8 (1999).

82. Hagedorn, C., Baiker, A., Postberg, J., Ehrhardt, A. & Lipps, H. J. Handling S/MAR vectors. *Cold Spring Harb Protoc* **2012,** 657–63 (2012).

83. Good, M. L., Vizcardo, R., Maeda, T., Tamaoki, N., Malekzadeh, P., Kawamoto, H. & Restifo, N. P. Using Human Induced Pluripotent Stem Cells for the Generation of Tumor Antigen-specific T Cells. *J Vis Exp* (2019).

84. García-Ojeda, M. E., Klein Wolterink, R. G. J., Lemaître, F., Richard-Le Goff, O., Hasan, M., Hendriks, R. W., Cumano, A. & Di Santo, J. P. GATA-3 promotes T-cell specification by repressing B-cell potential in pro–T cells in mice. *Blood* **121,** 1749–1759 (2013).

85. Dong, Y., Guo, H., Wang, D., Tu, R., Qing, G. & Liu, H. Genome-Wide Analysis Identifies Rag1 and Rag2 as Novel Notch1 Transcriptional Targets in Thymocytes. *Frontiers in Cell and Developmental Biology* **9** (2021).

86. Yu, S. *et al.* The TCF-1 and LEF-1 Transcription Factors Have Cooperative and Opposing Roles in T Cell Development and Malignancy. *Immunity* **37,** 813–826 (2012).

87. Arnold, M. *et al.* Global Burden of Cutaneous Melanoma in 2020 and Projections to 2040. *JAMA Dermatology* **158,** 495–503 (2022).

88. Janelle, V. & Delisle, J. S. T-Cell Dysfunction as a Limitation of Adoptive Immunotherapy: Current Concepts and Mitigation Strategies. *Cancers (Basel)* **13** (2021).

89. Nishimura, T. *et al.* Generation of Rejuvenated Antigen-Specific T Cells by Reprogramming to Pluripotency and Redifferentiation. *Cell Stem Cell* **12,** 114–126 (2013).

90. Varela-Rohena, A. *et al.* Genetic engineering of T cells for adoptive immunotherapy. *Immunol Res* **42,** 166–81 (2008).

91. Bozza, M. *et al.* Novel Non-integrating DNA Nano-S/MAR Vectors Restore Gene Function in Isogenic Patient-Derived Pancreatic Tumor Models. *Molecular Therapy - Methods Clinical Development* **17,** 957–968 (2020).

92. Hagedorn, C., Lipps, H. J. & Rupprecht, S. The epigenetic regulation of autonomous replicons. **1,** 17–30 (2010).

93. Rupprecht, S., Hagedorn, C., Seruggia, D., Magnusson, T., Wagner, E., Ogris, M. & Lipps, H. J. Controlled removal of a nonviral episomal vector from transfected cells. *Gene* **466,** 36–42 (2010).

94. Pan, G. & Thomson, J. A. Nanog and transcriptional networks in embryonic stem cell pluripotency. *Cell Research* **17,** 42–49 (2007).

95. Zhang, S. & Cui, W. Sox2, a key factor in the regulation of pluripotency and neural differentiation. *World J Stem Cells* **6,** 305–11 (2014).

96. Xing, S. *et al.* Tcf1 and Lef1 transcription factors establish CD8(+) T cell identity through intrinsic HDAC activity. *Nat Immunol* **17,** 695–703 (2016).

97. Dik, W. A. *et al.* New insights on human T cell development by quantitative T cell receptor gene rearrangement studies and gene expression profiling. *J Exp Med* **201,** 1715–23 (2005).

98. Wakabayashi, Y. *et al.* Bcl11b is required for differentiation and survival of αβ T lymphocytes. *Nature Immunology* **4,** 533–539 (2003).

99. Li, Q. *et al.* Comparison of the sorting efficiency and influence on cell function between the sterile flow cytometry and immunomagnetic bead purification methods. *Prep Biochem Biotechnol* **43,** 197–206 (2013).

100. Tajti, G., Szanto, T. G., Csoti, A., Racz, G., Evaristo, C., Hajdu, P. & Panyi, G. Immunomagnetic separation is a suitable method for electrophysiology and ion channel pharmacology studies on T cells. *Channels (Austin)* **15,** 53–66 (2021).

101. Petrie, H. T. & Zúñiga-Pflücker, J. C. Zoned Out: Functional Mapping of Stromal Signaling Microenvironments in the Thymus. *Annual Review of Immunology* **25,** 649–679 (2007).

102. Klein, L., Kyewski, B., Allen, P. M. & Hogquist, K. A. Positive and negative selection of the T cell repertoire: what thymocytes see (and don't see). *Nat Rev Immunol* **14,** 377–91 (2014).

103. Montel-Hagen, A. & Crooks, G. M. From pluripotent stem cells to T cells. *Experimental Hematology* **71,** 24–31 (2019).

104. Guo, R. *et al.* Guiding T lymphopoiesis from pluripotent stem cells by defined transcription factors. *Cell Research* **30,** 21–33 (2020).

105. Iriguchi, S. *et al.* A clinically applicable and scalable method to regenerate T-cells from iPSCs for off-the-shelf T-cell immunotherapy. *Nature Communications* **12,** 430 (2021).

106. Xu, H. *et al.* Targeted Disruption of HLA Genes via CRISPR-Cas9 Generates iPSCs with Enhanced Immune Compatibility. *Cell Stem Cell* **24,** 566–578.e7 (2019).

107. Gornalusse, G. G. *et al.* HLA-E-expressing pluripotent stem cells escape allogeneic responses and lysis by NK cells. *Nat Biotechnol* **35,** 765–772 (2017).

108. Lu, P. *et al.* Generating hypoimmunogenic human embryonic stem cells by the disruption of beta 2-microglobulin. *Stem Cell Rev Rep* **9,** 806–13 (2013).

109. Mandal, P. K. *et al.* Efficient ablation of genes in human hematopoietic stem and effector cells using CRISPR/Cas9. *Cell Stem Cell* **15,** 643–52 (2014).

110. Menon, A. P., Moreno, B., Meraviglia-Crivelli, D., Nonatelli, F., Villanueva, H., Barainka, M., Zheleva, A., van Santen, H. M. & Pastor, F. Modulating T Cell Responses by Targeting CD3. *Cancers* **15,** 1189 (2023).

111. Dong, D. *et al.* Structural basis of assembly of the human T cell receptor–CD3 complex. *Nature* **573,** 546–552 (2019).

112. Levelt, C. N. & Eichmann, K. Receptors and signals in early thymic selection. *Immunity* **3,** 667–672 (1995).

113. Van der Stegen, S. J. C. *et al.* Generation of T-cell-receptor-negative CD8αβ-positive CAR T cells from T-cell-derived induced pluripotent stem cells. *Nature Biomedical Engineering* **6,** 1284–1297 (2022).

114. Ciofani, M., Knowles, G. C., Wiest, D. L., von Boehmer, H. & Zúñiga-Pflücker, J. C. Stage-Specific and Differential Notch Dependency at the αβ and γδ T Lineage Bifurcation. *Immunity* **25,** 105–116 (2006).

115. Hayes, S. M., Li, L. & Love, P. E. TCR Signal Strength Influences αβ/γδ Lineage Fate. *Immunity* **22,** 583–593 (2005).

116. Ai, W., Li, H., Song, N., Li, L. & Chen, H. Optimal method to stimulate cytokine production and its use in immunotoxicity assessment. *Int J Environ Res Public Health* **10,** 3834–42 (2013).

117. Si, X., Xiao, L., Brown, C. E. & Wang, D. Preclinical Evaluation of CAR T Cell Function: In Vitro and In Vivo Models. *Int J Mol Sci* **23** (2022).

A Supplemental material

A.1 Surface expression of MCSP on human melanoma cell lines

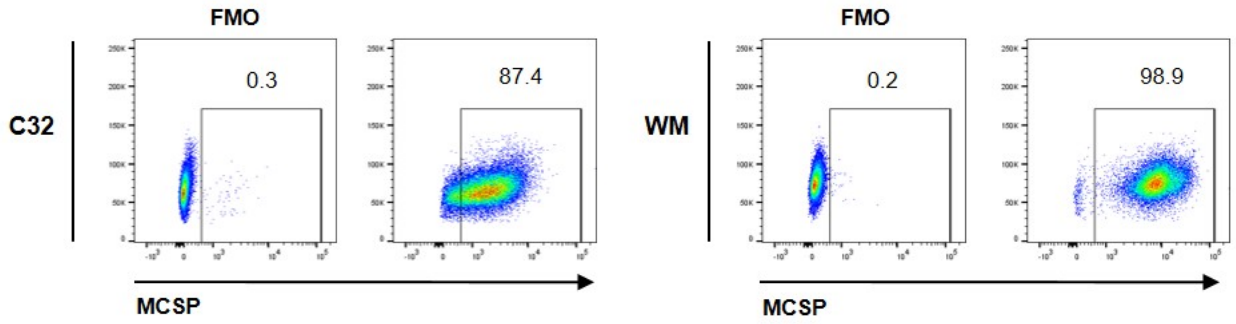

Fig. 18: Surface staining of MCSP on melanoma cell lines. Representative flow cytometry dot plots of C32 and WM266-4 melanoma cells after MCSP surface staining. Fluorescence Minus One (FMO) control was used to set the positive gates. Numbers indicate the percentage of MCSP positive cells from live cells.

A.2 HLA-A analysis for hiPSCs and melanoma cell lines C32 and WM266-4

Tab. 13: Sequencing results for the analysis of the HLA-A alleles

Cell line	**HLA-A (allele 1)**	**HLA-A (allele 2)**
hiPSC (HD11)	11:01:01G	68:01:02G
C32	01:01:01G	24:02:01G
WM266-4	02:01:01G	29:02:01G

Acknowledgement

Hereby I would like to thank everyone who helped and supported me during the time of my PhD. Without the help and support from all the people below, this work would not have been possible.

First, I would like to thank **Prof. Dr. Jochen Utikal** for giving me the great opportunity to conduct my PhD project in his group and for all the scientific support and guidance during the last years. I have learned so much during that journey and I will always remember not only the time in the lab but also the summer hikes and visits of the Christmas market.

Many thanks also go to **Prof. Dr. Viktor Umansky** for all his time and supervision. I am very grateful for his continual willingness to support and help, especially in questions related to immunology. A big thank you also goes to everyone from the Umansky group in Mannheim.

I also want to express my gratitude to my TAC members, **Prof. Dr. Adelheid Cerwenk**a and **Dr. Michael Milsom**, for all their suggestions and scientific input in my PhD project during the TAC meetings.

For the great time at the King's College London, I first and foremost want to thank **Dr. Pierre Guermonprez** for giving me the opportunity to learn more about hematopoiesis and FACS stainings. I also want to say thank you to the whole team in London, especially to **Giorgio, Pierre II, Roberto** and **Kristin** who have created such a friendly and enjoyable environment at the KCL.

I would also like to thank **Dr. Richard Harbottle** and his group for providing the vector systems and the scientific support in questions related to iPSC transfection and differentiation.

A big thank you goes to all the current and former members of A370 (G300). I really enjoyed working and spending time with you in and outside the lab. Starting with **Sunee, Tamara** and **Daniel**. I am so glad that I got the chance to meet and work with you. During the last years we spent so much time together and now we are not only colleagues anymore but friends who travel and discover the world (or Odenwald ;)) together. Having you on my side made everything much easier and more enjoyable.

A big "Thank you" also goes to the "old crew" **Karol, Laura** and **Nello** who welcomed me at the DKFZ in the beginning and made me feel like home not only in the lab but also in Heidelberg.

I am also grateful to **Marlene V** who taught me everything about iPSCs. Special gracias go to **Sandra** for taking over the project and for all the amazing moments we had together in the last year of my PhD.

For all the great time we spent together in and outside the lab I would also like to thank **Özge, Yiman, Nina** and **Mareike** as well as our technicians **Jenny, Marlene P** and **Diana**. It was always a big pleasure to have you on my site and I don't want to imagine all the years without you. I always enjoyed working and spending time with you. I am sure I will miss you all a lot!

Last but not least I wish to thank my whole family especially my **parents** and my **brother** and my **sister** for all their support and love not only during the last years but during my whole life. I love you, too!